Chapter 4

Electrochemistry and Spectroelectrochemistry of Homo- and Hetero-Dinuclear Ruthenium and Osmium Polypyridyl Complexes

*A series of binuclear ruthenium and osmium complexes $[(bipy)_2Ru(qpy)Ru(bipy)_2]^{4+}$ (**1**), $[(bipy)_2Os(qpy)Os(bipy)_2]^{4+}$ (**2**), $[(bipy)_2Ru(pytr\text{-}bipy)Ru(bipy)_2]^{3+}$ (**3**), $[(bipy)_2Ru(pytr\text{-}bipy)Os(bipy)_2]^{3+}$ (**4**), $[(bipy)_2Os(pytr\text{-}bipy)Ru(bipy)_2]^{3+}$(**5**) and $[(bipy)_2Os(bpbt)Os(bipy)_2]^{2+}$ (**6**) {bipy = 2,2′-bipyridyl; qpy = 2,2′:5′,5″:2″,2‴-quaterpyridyl; pytr-bipy = 3-(2,2′-bipyrid-6-yl)-5-(pyrid-2-yl)-1,2,4-triazolato, and bpbt = 5,5′-bis-(pyrid-2″-yl)-3,3′-bis-1,2,4-triazolato} are reported. Analysis of the electrochemical data focuses on structural factors and on determining the extent of electronic communication between the metal centres in the mixed valence oxidation state. Intervalence charge transfer (IT) bands could be identified in the spectra of the complexes **4** and **6** only. Analysis of their spectroelectrochemical data leads to the conclusion that the IT is superexchange mediated through the HOMO of the bridging ligand.*

4.1 Introduction

4.1.1 Supramolecular Chemistry

The world of science is driven by a great degree of ambition and an immense thirst to discover the unknown. Science as a subject has evolved into different disciplines and as a result of highly sophisticated approaches to research these disciplines are broken down and become more and more defined as time goes on. Over the last two centuries chemists have designed and successfully produced increasingly complex molecules held together by making and breaking covalent bonds.[1] With Alfred Werner's classification of coordination compounds at the turn of the 20th century came a new perspective on assembly of large complex molecules and the highly interdisciplinary field of supramolecular chemistry.

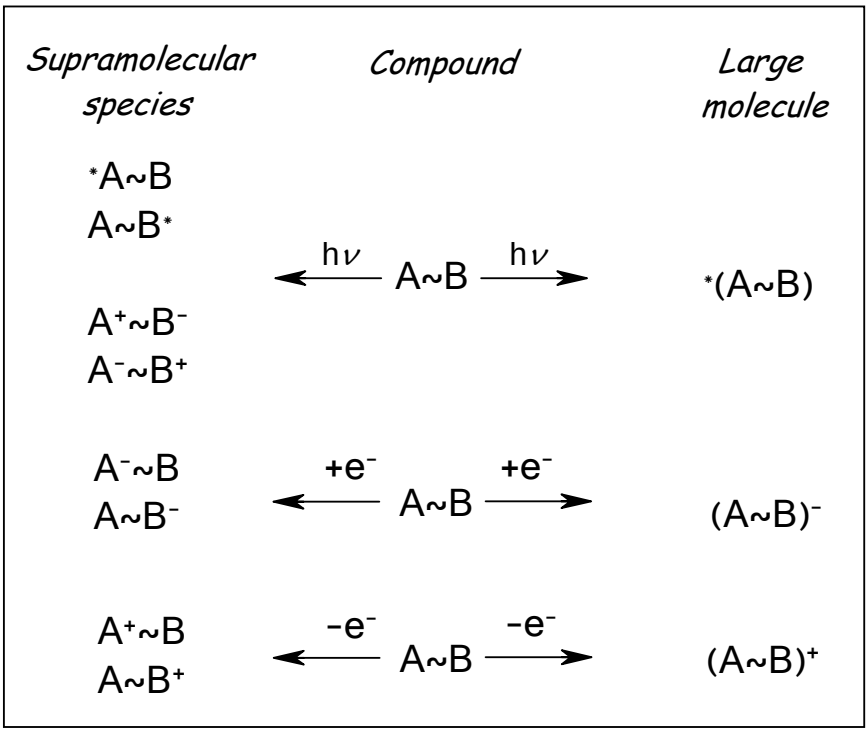

Figure 4.1: *Illustration of photochemical and electrochemical criteria used to classify a complex as a supramolecular species or a large molecule.*

It wasn't until the 1970's that this discipline was truly recognised and several definitions for supramolecular chemistry have been proposed; the most widely accepted being that by J.M. Lehn defining the area as "*the chemistry beyond the*

molecule, bearing on the organized entities of higher complexity that result from the association of two or more chemical species held together by intermolecular forces".[1, 2] These types of assemblies are created using molecular "building blocks" allowing the properties therein to be manipulated in a controlled manner.[3] In contrast to large molecules, supramolecular species are multicomponent or polynuclear systems that exhibit properties associated with those of the individual components as well as new properties related to the structure and composition of the entire array.[4]

Metal complexes based on polypyridyl ligands constitute versatile models for the construction of multifunctional supramolecular systems applicable in molecular photonics and molecular electronics.[5] The myriad of applications is founded on the well defined chemistry of these compounds and takes advantage of the favourable photophysical [6] and photochemical [7] and electrochemical [8] properties that are associated with the metal-to-ligand-charge-transfer (MLCT) excitation in these metal complexes.

4.1.2 Spectroelectrochemistry and Mixed Valence Systems

Metal-polypyridyl assemblies are characterized by the strong localization of redox processes within the complexes. The HOMO levels of ruthenium and osmium polypyridyl complexes are generally located on metal-centred orbitals with the LUMO levels known to reside on the ligands; oxidation and reduction sites are localized at the metal centres and at the pyridyl-based ligands, respectively. Oxidation of the ruthenium and osmium centres involves removal of an electron from the metal t_{2g} orbitals resulting in the low-spin $4d^5$ ($5d^5$ for osmium) configuration. This system is inert to ligand substitution resulting in a reversible redox process. The oxidation potential of the metal centres can be tuned by careful selection of the coordinated peripheral or bridging ligands. Those ligands with strong π-acceptor properties allow for back-bonding from the metal to the ligand stabilizing the t_{2g} orbitals. This increased stability leads to less electron density on the metal centre and as result the removal of an electron becomes difficult and the oxidation potential increases moving towards more positive potentials. As mentioned above, reducing the complexes result in addition of an electron to the LUMO localized on the ligands with the stable low-spin d^6 configuration remaining. In mixed ligand systems the first reduction will

occur on the ligand with the lowest lying π* orbital. Reduction of the triazole based ligands fall outside the potential window investigated due to the increased electron density and strong σ-donor character associated with these heterocycles.[9, 10]

As discussed above the main difference between conventional chemistry and supramolecular chemistry is that the latter moves away from the focus of the covalent bond and instead concentrates on the weaker bonds and interactions in complex molecules such as hydrogen bonding, electrostatic interactions, metal – metal communication etc. Spectroelectrochemistry is one of the many techniques used to analyse the weaker interactions in the molecule, in particular, the interaction between metal centres in transition metal complexes where any changes in the absorbance spectra are monitored when the complex is in the mixed valence. Amongst the many multinuclear polypyridyl complexes reported [4] an interesting subclass is represented by those binuclear systems that display additional spectroelectrochemical features due to the electronic interaction between the two metal centres in the mixed valence redox state(s).[11, 12]

Intramolecular interaction arising from direct orbital overlap of the metal centres would require an internuclear distance of a few Angstroms; any larger separation results in the interaction being purely electrostatic.[13] "Communication" between metal centres where direct orbital overlap is not possible is achieved through use of a bridging ligand (BL); it possesses a system of polarizable electrons that are capable of mediating the redistribution of the electronic charge as a result of the changes in the oxidation states of the two distinct metal centres.[13, 14, 15] Since bridging ligands are used as mediators between metal centres, their electronic properties play an important role: the position of the HOMO and LUMO levels of the bridge can determine whether a redistribution of charge from the donor to acceptor metals is achievable. The spatial orientation (length and configuration) of the BL will also influence the electron delocalization with the probability of charge transfer decreasing with increasing bridge length.[16] If the bridging ligand is sufficiently capable of mediating an internuclear interaction then direct (optical) electron transfer is possible in the mixed valence state (i.e., $M_1^{II}M_2^{III} \rightarrow M^{III}{}_1M^{II}{}_2$).[17, 18]

In supramolecular assemblies certain photochemical processes taking place between the individual components of the molecule are of particular importance as they can enhance the oxidising and reducing ability of a molecule. Such processes include those occurring following excitation by light (photoinduced electron and energy transfer) and those occurring directly upon excitation (optical electron transfer).[4]

Equation 4.1 $A \sim B + h\nu \rightarrow A^{+} \sim B^{-}$

Equation 4.2 $A \sim B + h\nu \rightarrow A^{*} \sim B \rightarrow A^{+} \sim B^{-}$

Equation 4.3 $A^{+} \sim B^{-} \rightarrow A \sim B$

Optical electron transfer (Equation 4.1) is a temperature independent form of electron transfer. Through use of electromagnetic radiation an electron is moved from the donor to the acceptor metal resulting in a charge separated species of opposite polarity to that of the initial mixed valence state.[13] For photoinduced and thermal electron transfer, thermal energy is necessary in order to transfer electronic charge, Equation 4.2. Thermal back electron transfer is a spontaneously thermodynamically favourable process which may follow optical or photoinduced electron transfer and is described in Equation 4.3. The relationship between each of these electron and energy transfer processes is illustrated in Figure 4.2.

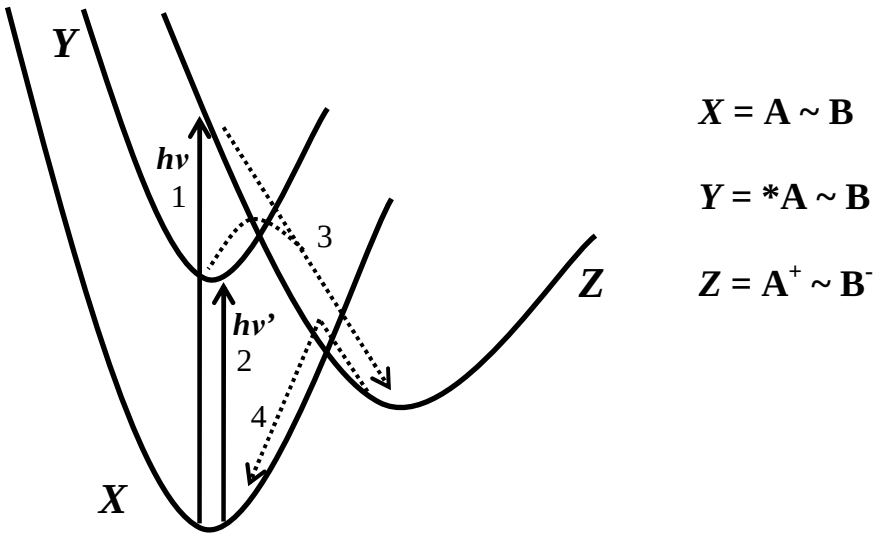

Figure 4.2: *Possible routes for electron transfer in a supramolecular species where 1 represents optical electron transfer, 2 and 3 represent photoinduced electron transfer and 4 represents thermal electron transfer.*

Following a vertical transition to the vibrationally excited state the nuclear coordinates of the product state equal that of the equilibrium geometry of the initial state (the rate of electron transfer is faster than nuclear motion so the nuclear geometry is effectively frozen) in accordance with the Franck Condon principle: this optical electron transfer is manifested in the appearance of metal-to-metal (MM'CT), or intervalence (IT) charge transfer, [19, 20a, 21] typically in the far red and near infrared region of the spectrum.[12, 14, 22] Analysis of these absorption bands [23] can provide detailed information as to the nature and extent of the interaction between the metal centres. The energy of such a transition, E_{op} encompasses not only the difference in Gibbs free energy of initial and final states, ΔG^o but also the reorganizational energy, λ according to the following expression

Equation 4.4 $$E_{op} = \lambda + \Delta G^o$$

For symmetrical systems Equation 4.4 becomes $E_{op} = \lambda$ because the value of ΔG^o is zero.

4.1.3 Interaction in the Mixed Valence State

Creating a mixed valence species results in a system that may be described as valence localized (M^{II}-M^{III}) or valence delocalized ($M^{II½}$-$M^{II½}$) depending on the extent of communication between the metal centres. Extensive study has been carried out on mixed valence systems and a theoretical basis for the study of intervalence transitions has been developed by Hush [20] Robin and Day [19] and later by Creutz, Meyer and others[17].

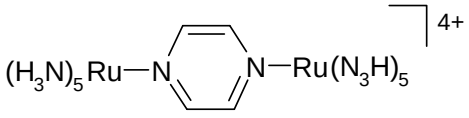

Figure 4.3: *Molecular structure of the Creutz Taube ion.*

Ligand bridged dinuclear ruthenium and osmium complexes have played an important role in the development of this theory; in particular the disclosure of the Creutz-Taube

ion (Figure 4.3), [24] where two ruthenium centres are bridged by a pyrazine ligand ($[(NH_3)_5Ru(pyr)Ru(NH_3)_5]^{4+}$), allowed for a greater understanding of the barriers to intramolecular electron transfer in these types of systems.

In the valence localized system (M^{II}-M^{III}) and (M^{III}-M^{II}) are considered electronic isomers in which a different equilibrium geometry exists for both. The reorganizational energy λ, the difference in energy between the two electronic isomers at their equilibrium geometry, consists of independent contributions from both inner and outer sphere effects. The inner sphere (λ_i) effects are concerned with the reorganisation of the metal-ligand and intra-ligand bond lengths and angles and the energy required for the re-orientation of the solvent around the metal centres constitutes the outer sphere (λ_o) effects.[20, 23a] When one of the electronic isomers is in a state of equilibrium, the other isomer can be considered as an electronically excited state, Figure 4.4. It is at this point that the opportunity for electron transfer arises and a transition from one state to the other is possible. The reorganizational energy, λ, is related to the intrinsic barrier to electron transfer, λ/4. At the point where one of the isomers can convert to the other, the energy and geometry of each is the same. As a result there are no Franck Condon restrictions to electron exchange and there is potential for thermal electron transfer.

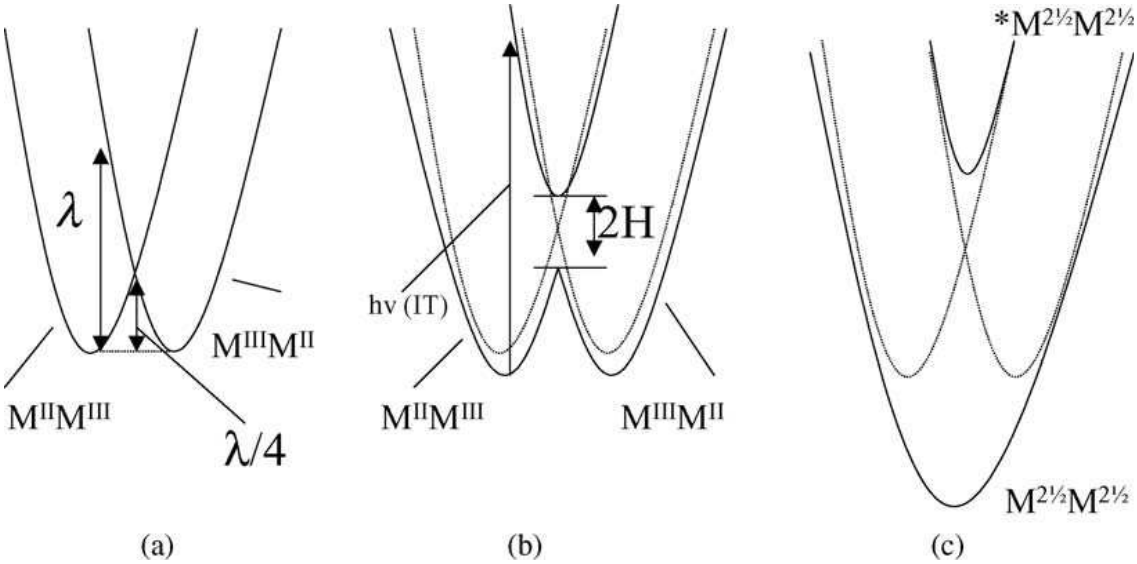

Figure 4.4: *Potential energy curves detailing the different types of interaction in mixed valence species: (a) negligible, (b) weak interaction and (c) strong interaction. The lighter grey, dashed lines represent the zero order states in (b) and (c).*[13]

In systems where the distance between the metal centres is large or the bridging ligand acts as an insulator between the metals then the electronic interaction (H_{ab}) between the two centres in the mixed valence state is negligible. This situation is known as Type I in the Robin and Day classification, [19] Figure 4.4a. The system may still gain the required activation energy to reach the intersection region of the diabatic curves however the probability of a transition is almost zero. The properties observed are those of the individual components within the complex as a whole. Type I systems may be characterized by the absence of an intervalence band in the absorbance spectra. It is also highly likely that a single redox wave will be observed in the cyclic voltammogram. The comproportionation constant will have the theoretical statistical limit of 4 (vide infra). An example of a Type I complex is that of the homonuclear ruthenium complex reported by Creutz in 1980, $[(bipy)_2(Cl)Ru(P2P)Ru(bipy)_2(Cl)]^{5+}$ (where P2P = 1,2-di-(pyryd-4'-yl)-ethane), Figure 4.5.[17] A single oxidation wave is observed representing the simultaneous oxidation of both metal centres. Also, the absence of IT bands in the infrared and near infrared region rule out any electronic coupling between the metal centres.[25]

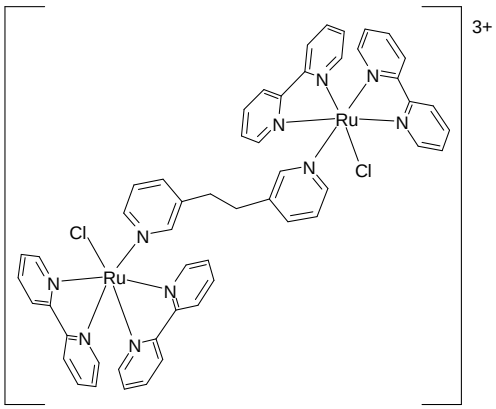

Figure 4.5: *Molecular structure of $[(bipy)_2(Cl)Ru(P2P)Ru(bipy)_2(Cl)]^{3+}$.*

For the majority of dinuclear complexes a certain degree of interaction and mixing of the potential wells occurs, either by direct overlap of the metal orbitals or indirectly using the orbitals of bridging ligand using a superexchange mechanism. Type II systems occur where there is a weak interaction between the metal centres in the mixed valence state. The effect of the interaction on the nuclear geometries is negligible in this case because the energy difference between the two electronic

isomers is much larger than H_{ab}. There is a certain degree of mixing of the zero-order states (Figure 4.4b). As a result of this the system will still possess some of the properties of its individual components as it is still considered valence localized but additional properties arise due to the ($M^{II}M^{III}$) interaction in the form of intervalence transfer transitions where $h\nu = \lambda$ and H_{ab} is only slightly smaller than $\lambda/4$ – the barrier to thermal electron transfer. This barrier to thermal electron transfer in Type II assemblies is only slightly less than the value calculated on the basis of the zero-energy curves, $\lambda/4$ (Figure 4.4a) and because of this only a weak interaction is observed. The intensity of the resulting intervalence bands observed in the absorbance spectra is heavily dependent on the degree of mixing of the two adiabatic states. Even though a certain degree of mixing of the two states occurs the system is best referred to as a valence localized ($M^{II}M^{III}$) with an example being that of $[(NH_3)_5Ru(P0P)Ru(NH_3)_5]^{5+}$ (where P0P = 4,4'-bipyridine) [17]. The effect of lengthening the bridging ligand on the electronic coupling between the centres is evident when comparing this system with the $[(NH_3)_5Ru(pz)Ru(NH_3)_5]^{5+}$, where pz = pyrazine. Using pyrazine as a bridging ligand results in a smaller distance between the metal centres and as a result the electronic coupling is greater and this complex is classed as a Type III system (*vide infra*).[17]

A third case arises when the bridging ligand allows for strong electronic coupling between the metal centres resulting in a large interaction. This causes a perturbation of the zero-order electronic state geometries and a new ground state minimum with an intermediate geometry realised where $H_{ab} \approx \lambda$, Figure 4.4c. These systems are best described as valence delocalized ($M^{2½}M^{2½}$) and are classed as Type III: the odd electron of the mixed valence state is located in an orbital that is evenly delocalized over the entire metal-bridge-metal system. The properties of the mixed valence state are generally unrelated to those of the individual components. The intervalence bands corresponding to the optical electron transfer between such strongly coupled centres are generally narrow intense absorption bands. Large comproportionation constants are associated with Type III systems indicating stable mixed valence species.

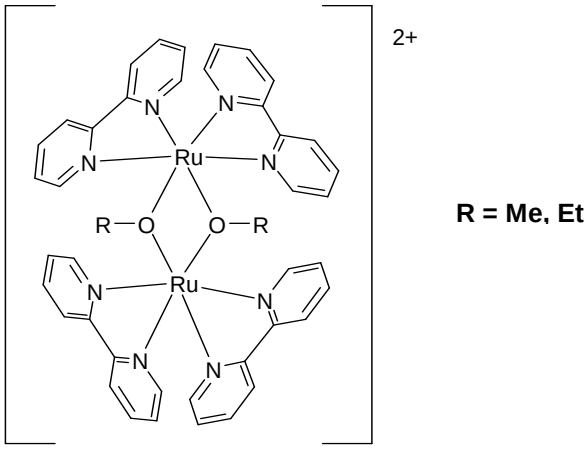

Figure 4.6: *Molecular structure of $[(bipy)_2Ru(OR)_2Ru(bipy)_2]^{2+}$.*

In 1993 Ward et al first published a strongly coupled homodinuclear ruthenium complex, $[(bipy)_2Ru(OR)_2Ru(bipy)_2]^{2+}$ (where R = Me or Et, Figure 4.6), exhibiting Type III behaviour.[26] Strong intervalence bands were observed for this complex suggesting that the alkoxide bridges are useful mediators for strong metal-metal interaction.

The Type III compounds fall into the "large molecule" category whereas Type I and Type II may be classified as supramolecular species. More recently there have been descriptions of complexes that possess properties of both Type II and Type III systems. As a result of this a fourth category exists to adequately describe the interaction in such complexes and these are referred to as simply Type II/III.[23a]

The extent of electron delocalization from the donor to the acceptor metal in the mixed valence state of dinuclear complexes can be calculated by analysing the properties of the intervalence band(s). Information detailing the extent of interaction can be obtained from such variables as the delocalization parameter, α^2, and the coupling constant, H_{ab}.

.

Equation 4.5 $$\alpha^2 = \frac{(4.2 \times 10^{-4})\varepsilon_{max}\Delta\nu_{1/2}}{d^2 E_{op}}$$

where ε_{max} is the extinction coefficient of the IT band ($M^{-1}cm^{-1}$), $\Delta\nu_{1/2}$ is the peak width at half height of the IT band (cm^{-1}), d is the distance between the metal centres (Å) and E_{op} is the energy of the IT band (cm^{-1}). For the series of complexes discussed in this chapter the distance *d* is taken to be 9.5 Å, [12d] however this value corresponds to the centre-to-centre distance and does not take into account the reduction in electron transfer distance due to strong mixing between metal orbitals and BL-based orbitals.[54] Hence the calculated values for α^2 and H_{ab} represent the lower limit of the actual value.

Equation 4.6 $H_{ab} = [\alpha^2 E_{op}^2]^{1/2}$

These two parameters are used to determine the strength of interaction between the two metal centres. The intensity of the intervalence band observed in the spectrum will depend on the degree of electronic coupling. Information about the class of interaction can be obtained from the theoretical peak width at half height, $\Delta\nu_{1/2calc}$. In cases where the value for the peak width at half height found from direct measurement of the IT band correlates well with the theoretical value obtained from Equation 4.7 then the system is best described as Type II (valence localized). If the IT band is narrower than that value predicted then the complex is a Type III valence delocalized system.

Equation 4.7 $\Delta\nu_{1/2calc} = [2310(E_{op} - \Delta E)]^{1/2}$

4.1.4 Electrochemistry and Comproportionation Equilibrium

Broadly speaking, mixed valence species [17, 18] can be generated electrochemically from both hetero- and homodinuclear [11c, 12a, 27, 28] complexes if the applied potential lies between the oxidation potentials of two metal centres: oxidation of one metal centre only leads to a decrease in electron density on that metal and as such the opportunity arises for "communication" between the two centres. In the more intriguing case of homodinuclear complexes, mixed valence species can be produced when the two equal metal centres coordinate ligands with considerably different donor

properties. Under these circumstances, the two metal centres are no longer equivalent electronically and their redox properties are thus distinguishable electrochemically.

For symmetrical dinuclear complexes any electronic coupling between the metal centres is presumed to result in a splitting in the oxidation potentials of the two metal centres; two metal centres undergoing oxidation at approximately the same potential indicating an absence in electronic coupling. K_c is the comproportionation constant and is used as an indication of the stability of the mixed valence [$M^{II}M^{III}$] species in relation to the fully reduced [$M^{II}M^{II}$] and fully oxidised [$M^{III}M^{III}$] forms.[23a] The peak-peak separation, ΔE (mV), is used to quantify the separation between the oxidation potentials of the two metal centres; K_c is directly proportional to ΔE and may be defined as the equilibrium constant for the reaction:

Equation 4.8 $$M^{II}M^{II} + M^{III}M^{III} \overset{K_c}{\rightleftharpoons} 2M^{II}M^{III}$$

for Type I and II systems and

Equation 4.9 $$M^{II}M^{II} + M^{III}M^{III} \overset{K_c}{\rightleftharpoons} 2M^{II½}M^{III½}$$

for Type III valence delocalized systems.

Equilibrium constants, like K_c for the above reactions, can be related back to the thermodynamic parameter of Gibbs free energy change for a system, ΔG and to the electrochemical properties using Equation 4.10.

Equation 4.10 $$\Delta G = -RT\ln K_c = -nF(\Delta E)$$

Equation 4.11 $$K_c = \exp[0.0389\Delta E] \qquad \text{at 298 K}$$

where ΔE is measured in mV.

Complexes where the interaction is strong yield large K_c values and complexes with little or no interaction, or symmetrical redox centres, give rise to small values for K_c. When the electronic interaction is negligible (Type I) a lower limit of 4 is assumed.[15] It is important to note however, that large K_c values often arise as a result of redox asymmetry in asymmetrical complexes and are not necessarily a direct measure of electrostatic interaction between metal centres. The comproportionation constant can be dependent on the conditions of the system; K_c can be particularly sensitive to the donor and acceptor strengths of the solvent and electrolyte and can vary as a result.[29] With this the electronic interaction and extent of electron delocalization can not be determined from electrochemical measurements alone.

4.1.5 Aim of this Chapter

In terms of molecular electronics, dinuclear complexes with two accessible, reversible redox centres assembled on a surface may be viable building blocks in the construction of molecular diodes for molecular electronic devices. The importance of the presence of electronic interaction in the mixed valence state of dinuclear complexes is, as of yet, uncertain in terms of realizing rectifying behaviour in these potentially useful systems. With this, the interaction in a series of dinuclear complexes has been analysed with the crucial factors for interaction examined also, *vide infra*.

The disclosure of the Creutz-Taube ion in 1969 [24] and the extensive analysis of its mixed valence state properties has led to increased interest into dinuclear mixed valence complexes and the extent and mechanisms of the interaction between the metal centres therein. In this chapter the electrochemical and spectroelectrochemical properties of a series of binuclear compounds of the general formula $M_1(bipy)_2$-BL-$M_2(bipy)_2$ where M represents a metal centre, bipy is 2,2'-bipiridyl, and BL is a bridging ligand are considered in order to evaluate the electronic communication between the two metal sites as a function of the electronic properties of the bridging ligand and the positioning of the two metal centres.

In particular, attention has been directed towards the homo- and heterodinuclear complexes of the d^6 metals ruthenium and osmium $[(bipy)_2Ru(qpy)Ru(bipy)_2]^{4+}$ (**1**), $[(bipy)_2Os(qpy)Os(bipy)_2]^{4+}$ (**2**), $[(bipy)_2Ru(pytr\text{-}bipy)Ru(bipy)_2]^{3+}$ (**3**),

$[(bipy)_2Ru(pytr\text{-}bipy)Os(bipy)_2]^{3+}$ (**4**), $[(bipy)_2Os(pytr\text{-}bipy)Ru(bipy)_2]^{3+}$(**5**), and $[(bipy)_2Os(bpbt)Os(bipy)_2]^{2+}$ (**6**) where bipy = 2,2'-bipiridyl, qpy = 2,2':5',5'':2'',2'''-quaterpyridyl, pytr-bipy = 3-(2,2'-bipyridyn-6-yl)-5-(pyridyn-2-yl)-1,2,4-triazolato, and bpbt = 5,5'-bis-(pyridyn-2''-yl)-3,3'-bis-1,2,4- triazolato (Figure 4.7). These compounds have been synthesised and characterised by Dr. Lynda Cassidy (Prof. J.G. Vos research group), the details of which have been reported previously.[30, 31]

The data are compared with the structures and spectroelectrochemical properties of the binuclear complexes $[(bipy)_2Ru(bpbt)Ru(bipy)_2]^{2+}$ (**7**), [12d] $[(bipy)_2Ru(bpt)Ru(bipy)_2]^{3+}$ (**8**), [12a, 28a] $[(bipy)_2Ru(bpt)Os(bipy)_2]^{3+}$ (**9**), [12e, 32] $[(bipy)_2Os(bpt)Os(bipy)_2]^{3+}$(**10**) [28b] and $[(bipy)_2Os(bpt)Ru(bipy)_2]^{3+}$ (**11**) [12e, 32] where bpt = 3,5-bis(pyridin-2'-yl)-1,2,4-triazole (Figure 4.7). The series of complexes $[(bipy)_2M(qpy_1)M(bipy)_2]^{4+}$ (**12**), $[(bipy)_2M(qpy_2)M(bipy)_2]^{4+}$ (**13**), and $[(bipy)_2M(qpy_3)M(bipy)_2]^{4+}$ (**14**) with qpy_1 = 2,2':3',2'':6'',2'''-quaterpyridyl [7, 14a, 33], qpy_2 = 2,2':4',4'':2'',2'''-quaterpyridyl [34, 35], qpy_3 = 2,2':4',2'':6'',2'''-quaterpyridyl [36] (Figure 4.8), are compared with the photophysical and electrochemical properties of the homonuclear $[(bipy)_2Ru(qpy)Ru(bipy)_2]^{4+}$ (**1**) and $[(bipy)_2Os(qpy)Os(bipy)_2]^{4+}$ (**2**) described here. Of particular emphasis is the effect of the differences in connectivity between the bridging ligands. The systematic variation in the nature of the bridge and the introduction of both ruthenium and osmium metal centres allows a critical evaluation of the structural factors that affect the extent of electronic communication between the metal centres of these types of dinuclear complexes.

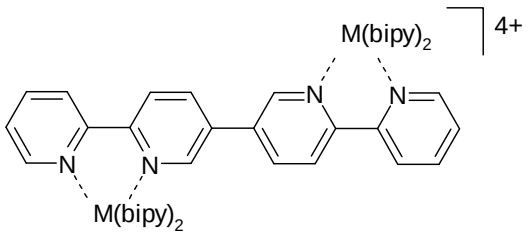

1: M = Ru
2: M = Os

bipy : 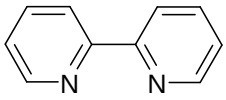

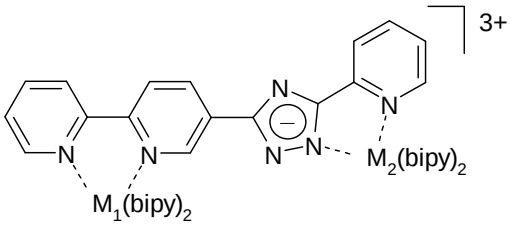

3: M_1=M_2 = Ru
4: M_1= Os; M_2 = Ru
5: M_1= Ru; M_2 = Os

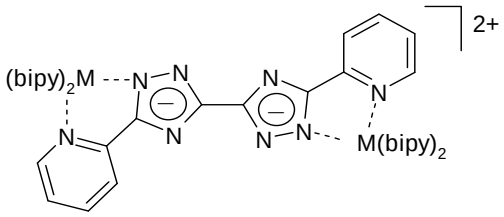

6: M = Os
7: M = Ru

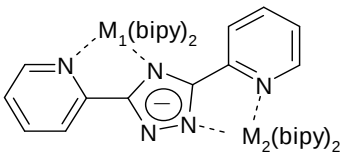

8: M_1= M_2 = Ru
9: M_1= Os; M_2 = Ru
10: M_1= M_2 = Os
11: M_1= Ru; M_2 = Os

Figure 4.7: *Structures of new binuclear complexes **1-6** reported here and the reference homo- and heterodinuclear ruthenium/osmium complexes **7-11**.*

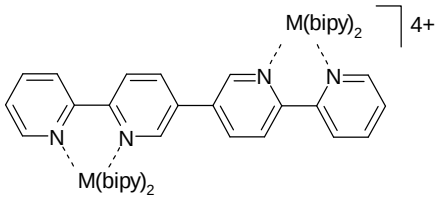

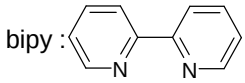

1: M = Ru
2: M = Os

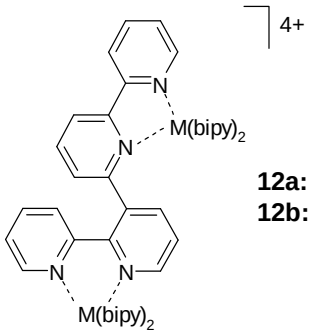

12a: M = Ru
12b: M = Os

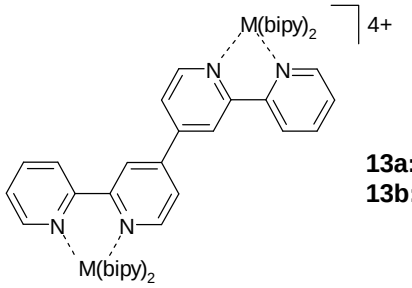

13a: M = Ru
13b: M = Os

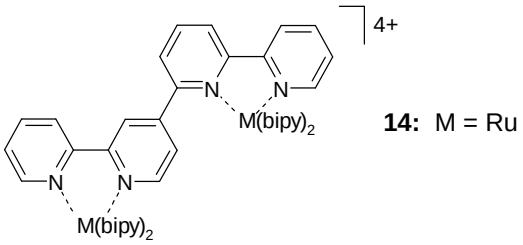

14: M = Ru

Figure 4.8: *Structures of quaterpyridyl bridged binuclear complexes **1**, **2**, $[(bipy)_2M_1(qpy_1)M_2(bipy)_2]^{4+}$ **(12)**, $[(bipy)_2M(qpy_2)M(bipy)_2]^{4+}$ **(13)**, and $[(bipy)_2M(qpy_3)M(bipy)_2]^{4+}$ **(14)** differing for the isomer type of quaterpyridine BL.*

The electrochemical and spectroelectrochemical properties of complexes **7** – **11** have been examined by Vos *et al*.[12a, d and e, 28, 32] It is revealed that in all five complexes the metal centres are oxidised at independent redox potentials. This observation and the

presence of IT bands in the absorbance spectra indicate the presence of electronic interaction between the metal centres in the mixed valence state. The presence of the triazole unit on the bridging ligand has proved to play an important role in the investigation of intercomponent interaction in these dinuclear systems. Triazole rings offer synthetic flexibility which in turn allows for the tuning of the electronic and electrochemical properties.

Coordination of the triazole ligand to a metal centres leads to deprotonation of the ring: the loss of this proton destabilizes the σ-orbitals of the bridge to a certain extent which is a significant aspect of intermetallic "communication" in the mixed valence state. It is suggested that the delocalization of electron density from the donor to the acceptor metals in the mixed valence state occurs via a HOMO mediated superexchange mechanism: electron transfer occurs via mixing of the metal based HOMO levels (dπ-orbitals) with the HOMO levels of the bridging ligand (σ-orbitals). When the bridge is protonated the σ-orbitals of the triazole ring are stabilized and this leads to an increase in the energy gap between the metal and bridging ligand HOMO levels and a concurrent decrease in interaction between the metal centres.[12, 13]

The elucidation of the electron transfer mechanism as a HOMO mediated superexchange is further supported by the dinuclear $Ru^{II}(bipy)_2$ complex bridged by 1,2,4-triazole-3,5-dicarboxylic acid as reported by Nag *et al.* in 2004.[37] The increased electron withdrawing properties of the carboxylic acid groups leads to a stabilisation of the σ-orbitals of the triazole unit as a result of less electron density on the ring. The peak - peak separation in the cyclic voltammetry of the complex is reduced and as a result the interaction between the metal centres is decreased.

The presence of the negative charge on the bridging ligand proves to be an important factor in the realisation of electronic delocalization between metal centres in the mixed valence state. Complexes **12** – **14** are bridged by quaterpyridyl ligands possessing strong π-acceptor properties. Disrupting the conjugation of the π subunits across the quaterpyridyl bridge will affect the electronic interaction. This was demonstrated by Steel *et al*. [34] in 1991 where the ability of the two bridging bipy units to rotate around the C4'-C4" bond led to a reduced coupling between the metals and the resulting interaction was, at best, very weak.

Likewise in 2003, Hanan *et al.* [35] reported a series of homo- and heterodinuclear complexes bridged by a quaterpyridyl unit connected at the C4'-C4" position also. Like that of Steel *et al.* a very weak metal – metal interaction was reported. This was observed through a favourable comparison of the oxidation potentials of the metal centres in the dinuclear complexes with those of the mononuclear subunits. The lack of coupling across the quaterpyridyl bridge is further supported in the all ruthenium dimer published by Ward in 1993.[36] Two very closely spaced oxidations of the complex were observed indicating a weak electrostatic interaction across the bridge.

4.2 Results and Discussion

4.2.1 Redox Properties

The redox properties of dinuclear complexes **1-6** have been investigated using cyclic voltammetry and differential pulse voltammetry, the results of which are detailed in Table 4.1.

	$E_{1/2\ ox}$ / V *vs* SCE	ΔE_p / mV	$E_{1/2\ red}$ / V *vs* SCE
1	+1.34	70	-1.01 [BL], -1.20 [BL], -1.50, -1.80
2	+0.89	60	-0.99 [BL], -1.16[BL], -1.47, -1.77
3	+0.99, +1.36	70, 70	-1.32 [BL], -1.50, -1.76
4	+0.86 (Os), +0.97 (Ru)	50, 60	-1.24 [BL], -1.47, -1.81
5	+0.56 (Os), +1.31 (Ru)	60, 70	-1.30, -1.40, -1.52, -1.70, -1.82 [BL]
6	+0.47, +0.56	40, 40	-1.42, -1.70
7 [12d]	+0.80, +0.98		-1.22, -1.53, -1.70
8 [12a, 28a]	+1.04, +1.34		-1.40, -1.62, -1.67, -2.23
9 [12e, 32]	+0.73(Os), +1.20(Ru)		-1.33, -1.41, -1.59, -1.69, -2.15, -2.32
10 [28b]	+0.64, +0.85		-1.34, -1.57, -2.23, -2.30
11 [12, 32]	+0.65(Os), +1.30(Ru)		-1.36, -1.63, -2.17, -2.32
12a [38]	+1.33, +1.44		-1.15, -1.36, -1.58
12b [33b]	+0.97, +1.06		-0.98, -1.22, -1.40
13a [34]	+1.24	85	-1.10, -1.44, -1.57, -1.64
13b [35]	+1.28	92	
14 [36]	+1.30, +1.47		-1.05, -1.32, -1.45
$[Ru(bipy)_3]^{2+}$ [39]	+1.26		-1.35, -1.55, -1.80
$[Os(bipy)_3]^{2+}$ [40]	+0.83		-1.28

Table 4.1: *Cyclic voltammetric data of complexes **1-6** and related compounds: formal potential, $E_{1/2}$ [$E_{1/2} = (E_{p,a}+E_{p,c})/2$], and peak separation, ΔE_p ($\Delta E_p = |E_{p,a}-E_{p,c}|$). E_{pa} and E_{pc} are the potential values corresponding to the anodic and cathodic peaks, respectively. BL =bridging ligand.*

The half-wave potentials, $E_{1/2}$ as determined by cyclic voltammetry indicate that the oxidations and reductions of each of the six complexes are centred on the metals and ligands, respectively.[8] For homodinuclear complexes **1** and **2**, a single reversible metal oxidation wave is observed and assigned to two one-electron oxidations of the two metal centres M(II)→M(III). The oxidation process Ru(II)→Ru(III) in **1** is at more positive potentials with respect to Os(II)→Os(III) in **2** [1.34 *versus* 0.89 V *vs* SCE (Table 4.1)] due to the destabilization of the osmium 5d orbitals compared to the 4d orbitals of ruthenium.[22, 41]

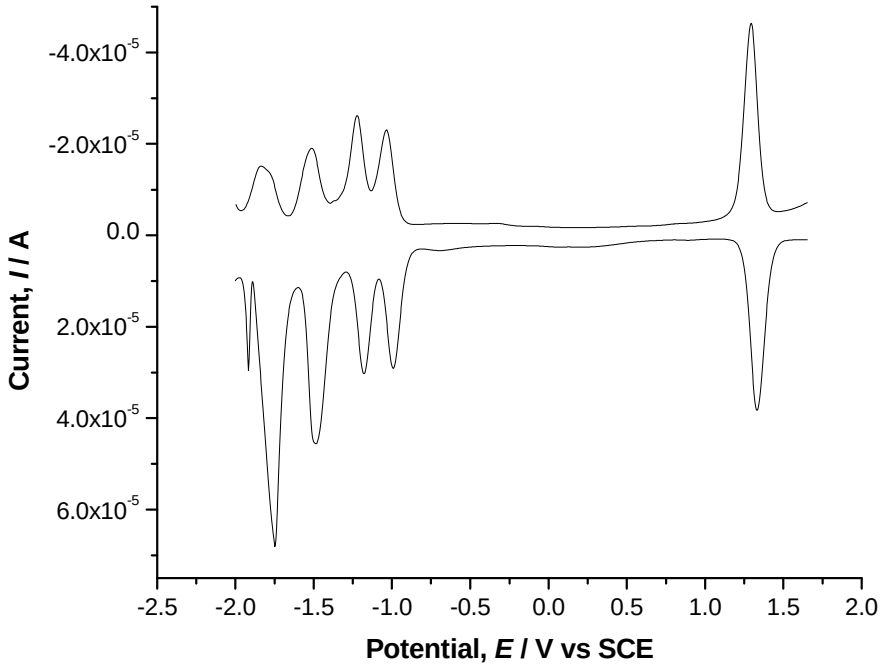

Figure 4.9: *Differential pulse voltammogram of complex **1** [1mM], at a glassy carbon electrode (3 mm geometrical diameter), in acetonitrile:dichloromethane (1:1) with 0.1 M $TBAPF_6$ as the supporting electrolyte.*

The symmetric homodinuclear complex **1** exhibits electrochemical properties (Figure 4.9) similar to that of its regioisomer $[Ru(bipy)_2(qpy)Ru(bipy)_2]^{4+}$ (**13a**) first reported by Steel *et al.*[26] in which the bipyridyls of the BL are connected at the C4 position. A reversible two electron oxidation wave at +1.34 V is observed for **1**, i.e. 100 mV more positive than the oxidation potential reported for **13a**.[26] This difference is assigned to the variation in connectivity of the two bipyridyl moieties of the BL. **13a** is linked at

the C4-C4' position allowing for rotation around the C-C bond whereas direct linkage from C5 in **1** leads to a more impeded rotation around the bond. This would diminish delocalisation across the bridge with consequent increase in the oxidation potential for the bridged metal centres in **1** compared to **13a**. The ΔE_p of 70 mV for **1** (Table 4.1) is larger than the theoretical value expected for a reversible one-electron process of 59 mV,[42, 43] however the ratio of the peak currents (= 0.93) clearly indicates the reversibility of the oxidation.

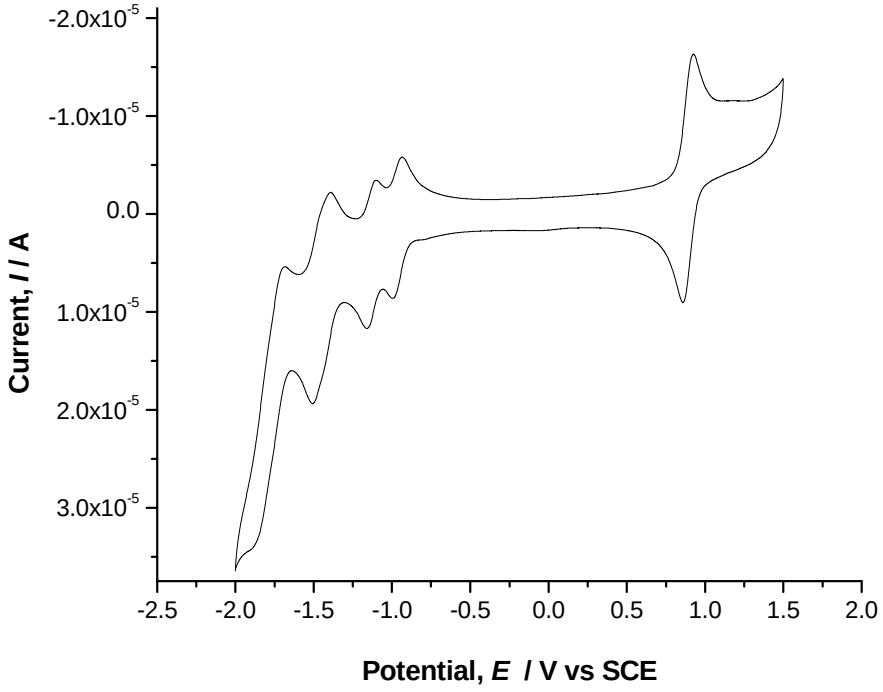

Figure 4.10: *Cyclic voltammogram of complex **2** [1mM], at a glassy carbon electrode (3 mm geometrical diameter), in acetonitrile:dichloromethane (1:1) with 0.1 M $TBAPF_6$ as the supporting electrolyte. Scan rate: 100 mV/s.*

The electrochemistry of the osmium analogue **2** (Figure 4.10) is similar to that of **1** with the observation of one anodic process and four cathodic processes. A difference of 440 mV between the anodic half-wave potentials of **1** and **2** is observed which is expected for osmium compounds when compared to their ruthenium analogues.[9] The redox potential of $[Os(bipy)_3]^{2+}$ is +0.83 V *vs* SCE [40] which is 60 mV lower than the redox potential of Os in **2**. Both osmium metal centres are oxidised simultaneously

and only one reversible anodic wave is observed representing two one-electron processes. This suggests that electronic interaction between the two metal centres is negligible. Four cathodic processes are resolved in the CV of **1** and **2**, and analysis by differential pulse voltammetry (DPV) indicates that these four redox waves correspond to six reduction steps with only the first two redox processes being fully resolved, Figure 4.9.

Comparison with related compounds and considering π-acceptor properties of the BL, suggests that the first two reductions at -1.00 and -1.20 V *vs.* SCE are localized on the BL rather than on the peripheral bipyridyl ligands.[34, 44] The third and fourth reduction waves, each representing two partially resolved one-electron reductions, are assigned to the reductions of the four peripheral bipyridyl ligands. The comparison of the reduction potential values for the quaterpyridyl BL in complexes **1** and **2** shows a weak dependence of these on the nature of the coordinating metal.

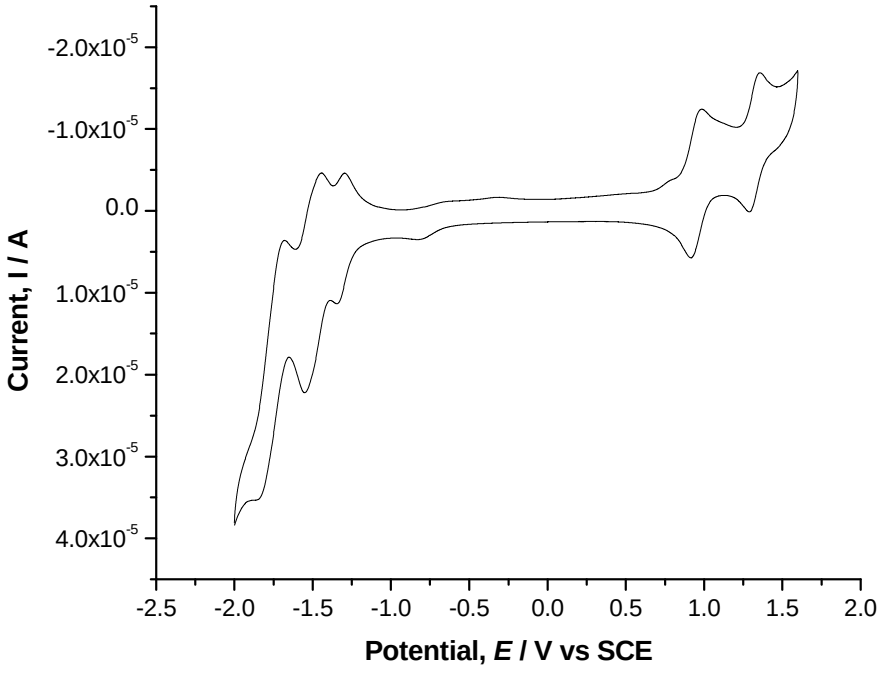

Figure 4.11: *Cyclic voltammogram of complex* $[(bipy)_2Ru(pytr\text{-}bipy)Ru(bipy)_2]^{3+}$ ***3*** *[1mM], at a glassy carbon electrode (3 mm geometrical diameter), in acetonitrile:dichloromethane (1:1) with 0.1 M* $TBAPF_6$ *as the supporting electrolyte. Scan rate: 100 mV/s.*

In contrast to **1** and **2**, homodinuclear ruthenium complex **3** exhibits two well resolved reversible one-electron oxidation waves (Figure 4.11) that correspond to the sequential oxidations at the two different binding sites of the asymmetric ditopic pytr-bipy bridging ligand. The two redox processes can be assigned to oxidation of metal centres coordinated to the pytr (+0.99 V *vs.* SCE) and bipy (+1.36 V *vs.* SCE) components of the BL, respectively, by comparison with the redox potentials of related complexes.[6a, 12d,e, 40, 45] The introduction of a triazole moiety to the bridging ligand accounts for this negative shift in the former with respect to complex **1** since the negatively charged triazolato groups exhibit stronger σ-donor properties and are weaker π-acceptor ligands relative to the bipyridine ligand. In the case of the bridging ligand in **3** the stronger donor properties are displayed by the N1 atom of the triazole moiety with respect to N4 in the same ring, and to the nitrogen of the pyridine sub-unit.[6a, 12d, 12e] The similarity of the latter redox potential with that of complex **1** is an indication of the localisation of this oxidation process at the metal centre that coordinates the bipyridyl unit of the BL. This potential is 100 mV higher than the oxidation potential of the mononuclear complex $[Ru(bipy)_3]^{2+}$, Table 4.1.[33a] This positive shift may be a consequence of electronic effects since the $Ru(bipy)_2(bipy)^{2+}$ moiety in complex **3** is close to the positively charged moiety obtained upon oxidation of the Ru centre bonded to the triazole moiety of the BL.

The least negative, one-electron, reduction process at -1.32 V is assigned to reduction of the bipy grouping on the pytr-bipy ligand of **3**, Figure 4.11. This is because the number of exchanged electrons at −1.32 V corresponds to a process of mono-electronic reduction. Therefore, this implies the involvement of a bipy unit belonging to the BL in **3**. If reduction would have taken place at a peripheral bipy, the number of exchanged electrons would have been two, as for the reduction process occurring at lower potential values. The two redox waves at more negative potentials (−1.50 and −1.76 V *vs.* SCE, Figure 4.11) are assigned to the first and second reduction of the peripheral bipy ligands, respectively. The second reduction step of the triazole based ligand lies outside the potential window available. Similar assignments can be made in the analysis of the reduction processes of the same BL in heterodinuclear complex **4** (Table 4.1).

The oxidation processes of the heterodinuclear complexes **4** and **5** consist of two resolved one-electron redox steps, the separation of the two redox waves being markedly different between the two complexes (Figure 4.12). The Ru oxidation potential is shifted towards more positive potentials in passing from complex **4** in which Ru coordinates the pyridyl-triazole moiety of the BL, to **5** in which the same metal coordinates the bipyridyl moiety of the BL. Such a positive shift is expected due to the decrease of the σ-donor properties of the coordinated nitrogen when passing from the triazole ring to the pyridyl sub-unit.[12d, 12e] For **5**, assignment of the two redox processes can be made on the basis of comparison with related mononuclear complexes. The first oxidation is assigned to the pyridyl-triazolato bound osmium centre (+0.56 V) while the second process at +1.31 V is assigned to the ruthenium centre bound to the bipyridyl unit of the bridging ligand.

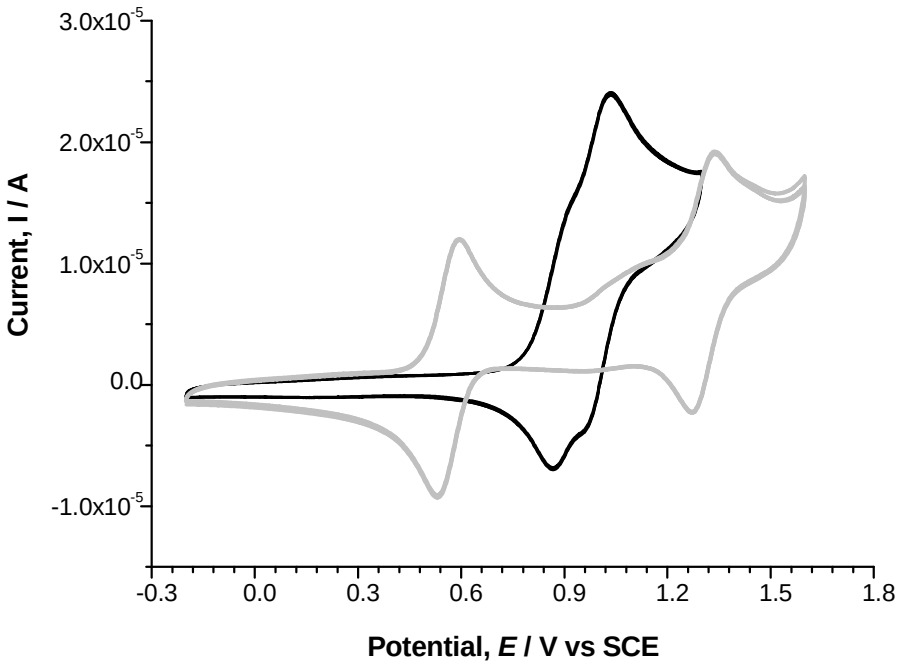

Figure 4.12: *Cyclic voltammograms of the anodic processes of $[(bipy)_2Ru(pytr\text{-}bipy)Os(bipy)_2]^{3+}$(**4**) (black) and $[(bipy)_2Os(pytr\text{-}bipy)Ru(bipy)_2]^{3+}$(**5**) (grey) [1mM], at a glassy carbon electrode (3 mm geometrical diameter), in acetonitrile:dichloromethane (1:1) with 0.1 M $TBAPF_6$ as the supporting electrolyte. Scan rate: 100 mV/s.*

For **4**, the assignment is less obvious since the two redox waves are separated by only 110 mV and are both close to those of their related mononuclear complexes. Assignment on the basis of comparison would suggest that the $Os(bipy)_2$-bipyridyl bound centre is the first to be oxidised followed by the $Ru(bipy)_2$-pyridyl-triazolato centre. This assignment is verifiable by spectroelectrochemistry (*vide infra*) which shows that the first oxidation is accompanied by a decrease in the intensity of the osmium ^{3}MLCT absorption bands. Overall, the difference in the half–wave potentials of the ruthenium and osmium metal centres is small in complex **4** ($\Delta E_{1/2}$, 110 mV) compared to that observed for complex **5** ($\Delta E_{1/2}$, 750 mV), Figure 4.12.

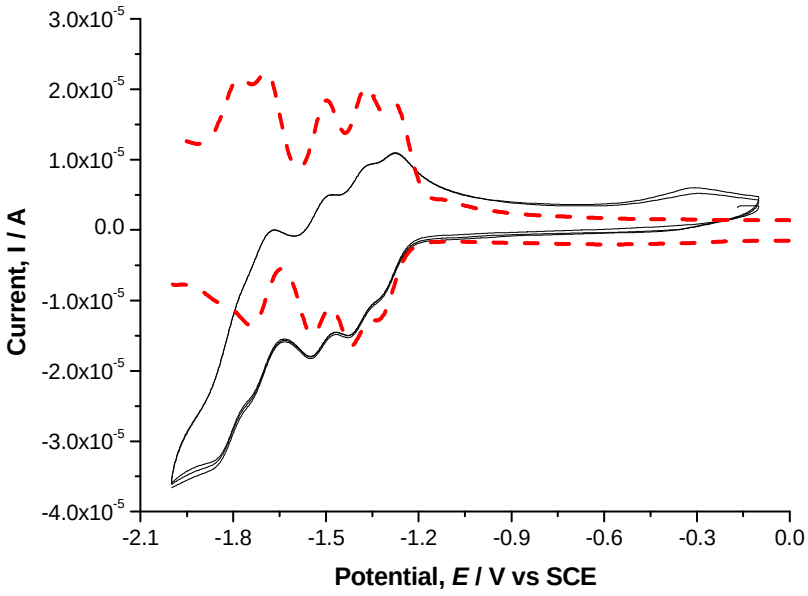

.

Figure 4.13: *Cyclic voltammogram (black full line) and differential pulse voltammetry (dotted red line) of the cathodic processes of $[(bipy)_2Os(pytr\text{-}bipy)Ru(bipy)_2]^{3+}$(**5**) [1mM], at a glassy carbon electrode (3 mm geometrical diameter), in acetonitrile:dichloromethane (1:1) with 0.1 M $TBAPF_6$ as the supporting electrolyte. Scan rate: 100 mV/s.*

Analysis of the reduction processes with cyclic voltammetry and differential pulse voltammetry in heterodinuclear $[(bipy)_2Os(pytr\text{-}bipy)Ru(bipy)_2]^{3+}$ (**5**) (Figure 4.13), shows five distinct one-electron processes. In analogy to $Ru(bipy)_3$, the reduction peaks at -1.30 V and -1.52 V are assigned to the reduction of the two non-bridging

bipy ligands that are coordinated by Ru(II) in **5**. Similarly, the two reduction steps at -1.40 V and -1.70 V are still ascribed to the reduction of the two non-bridging bipy ligands that are coordinated by Os(II). The negative shift observed for the reduction steps of the non-bridging ligands of Os(II) is related to the presence of a negative charge in the triazolato moiety coordinated by Os(II), and secondly, the stronger electron releasing properties of Os(II) with respect to Ru(II). The fifth reduction step at -1.82 V is assigned to the reduction of the BL in correspondence of the bipy moiety of the BL because of the closeness of this value with that of the third reduction potential of $Ru(bipy)_3$, Table 4.1.

Since triazoles are stronger σ-donors (and hence weaker π-acceptors) than bipyridyl ligands, they are reduced at more negative potential values. Consequently, the reduction potential of pytr moieties falls outside the potential window investigated here (-2.0 to +1.6 V).

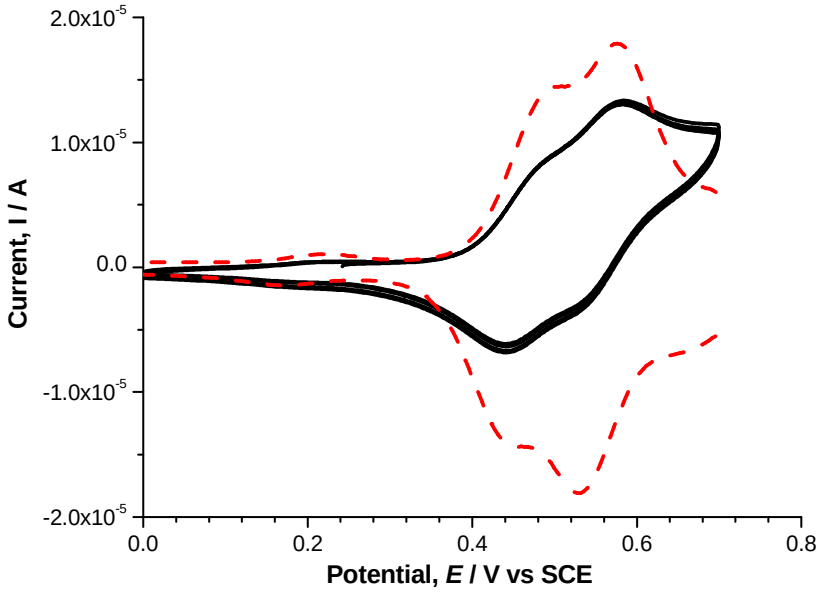

Figure 4.14: *Cyclic voltammogram (black full line) and differential pulse voltammetry (dotted red line) of the anodic processes of* $[(bipy)_2Os(bpbt)Os(bipy)_2]^{2+}$ ***(6)*** *[1mM], at a glassy carbon electrode (3 mm geometrical diameter), in acetonitrile:dichloromethane (1:1) with 0.1 M* $TBAPF_6$ *as the supporting electrolyte. Scan rate: 100 mV/s.*

Complex **6**, the osmium analogue of $[(bipy)_2Ru(bpbt)Ru(bipy)_2]^{2+}$ [12d] exhibits two reversible one-electron oxidations at $E_{1/2}$ = +0.47 and +0.56 V *vs.* SCE (Table 4.1 and Figure 4.14). The metal centres in **6** are oxidised at less positive potentials than the sites in the ruthenium analogue as a consequence of the less rigid, more polarizable electrons in the 5d orbitals of osmium. Despite the chemical equivalency of the Os sites in neutral **6** (Figure 4.7), two close, but resolved redox waves appear for the oxidation of the two metal centres, Figure 4.14.

Interestingly the analogous ruthenium complex $[(bipy)_2Ru(bpbt)Ru(bipy)_2]^{2+}$ has a ΔE value of 180 mV, i.e. twice that observed for **6**. The first metal oxidation potential of **6** is 420 mV lower than the oxidation potential of the metal centres in the homodinuclear osmium complex **2** in agreement with the coordination of both metal centres to pyridyl-triazolato units. The two reduction waves of complex **6** are consistent with two bi-electronic processes of reduction that are localised on bipy ligands as reported previously.[12, 46]

4.2.2 Comproportionation Constant as a Measure of Intermetallic Interaction

With the exclusion of homodinuclear complexes **1** and **2**, the observation of a separation in the oxidation potentials of the metals indicates either electrostatic interaction (through space effect) or ligand-mediated delocalisation of the SOMO over both metals. As mentioned above, the comproportionation constant, K_c (Equation 4.11) can be calculated from the difference in potentials of each metal centre: $\Delta E = \left| E_{1/2}(M_1) - E_{1/2}(M_2) \right|$.[47]

The comproportionation constant, K_c, calculated from the ΔE values according to Eq. 1, is a useful indicator of the extent of electrostatic interaction and redox asymmetry between the metal centres as well as the stability of the mixed valence compound.[13, 15] The comproportionation constants for complexes **1** – **14**, referring to the above equilibrium, are reported in Table 4.2. The largest K_c values in this series of complexes are observed for complexes **3** and **5** with calculated values of 1.8×10^6 and 4.8×10^{12} for ΔE = 370 (**3**) and 750 (**5**) mV, respectively. Complexes **4** and **6** present

lower values of ΔE (110 and 90 mV, respectively), and hence K_c is 72 (**4**) and 35 (**6**), respectively.

	$\Delta E \pm 30$ / mV	K_c
1	0	~ 4
2	0	~ 4
3	370	$1.8*10^6$
4	110	72
5	750	$4.8*10^{12}$
6	90	35
7 [12d]	180	1100
8 [12e]	300	$1.2*10^5$
9 [12e]	470	$8.9*10^7$
10 [12e]	210	$3.6*10^3$
11 [12e]	650	$9.9*10^{11}$
12a [38]	110	72
12b [33b]	90	35
13a [34]	0	~ 4
13b [35]	0	~ 4
14 [36]	170	744

Table 4.2: *Separation between first and second oxidation potentials, ΔE, and the corresponding comproportionation constant, K_c (Equation 4.11), for dinuclear complexes **1**-**14**.*

In dinuclear complexes where ΔE = 0 mV and the redox sites are then electrochemically equivalent, the limiting value of K_c is 4, which corresponds to the statistical value.[17] With this limiting situation the fully reduced ($M^{II}M^{II}$) and fully oxidised ($M^{III}M^{III}$) forms each account for 25 % of the mixture with the mixed valence ($M^{II}M^{III}$) species making up the other 50 %.[26b] In the case of the complexes **1** and **2**,

the concurrent oxidation of both metal centres indicates that the electronic coupling across the bisbipyridyl bridge is either absent or weak and that an electrostatic interaction is absent.[4] This conclusion is supported by the absence of an intervalence transfer band in the vis–NIR spectrum of these systems (*vide infra*).

Generally, the observation of a separation between the metal centred oxidation potentials is taken as an indication of electrostatic interaction or ligand orbital mediated superexchange between the metal centres. It is important, however, to note that the nature of the metal centres involved also plays a role. The related comproportionation constant, K_c (*vide supra*), calculated using ΔE (Equation 4.11), is therefore often taken as an indicator of the extent of electrostatic interaction and thermodynamic stability of the mixed valence compound as well as redox asymmetry between the metal centres in the case of asymmetric complexes (Table 4.2).[13, 14, 15, 47] Since absorption bands assignable to IT transitions were observed for complexes **4** and **6** whereas compounds **3** and **5** showed no evidence of such absorptions (*vide infra*), the value of K_c observed for these compounds reduces to be that of a measure of the redox asymmetry between the metal centres and/or to the degree of electrostatic interaction. It must also be taken into account that the value of K_c is sensitive to the donor/acceptor properties of solvent and electrolyte, and varies as a result.[29]

4.2.3 Spectroelectrochemistry - Oxidative

The spectral properties of the binuclear complexes **1**-**6** are summarized in Table 4.3. The absorption bands in the UV are assigned to $\pi \rightarrow \pi^*$ intraligand electronic transitions (wavenumber range: $\overline{\nu} > 25000$ cm^{-1} for polypyridyl-based ligands).[48] The absorption bands detected in the wavenumber range $13850 < \overline{\nu} < 23800$ cm^{-1} ($420 < \lambda < 720$ nm) are assigned to MLCT transitions. The homodinuclear complexes of Ru, **1** and **3**, show singlet-based ^{1}MLCT type transitions in the range $21250 < \overline{\nu} < 24000$ cm^{-1} ($420 < \lambda < 470$ nm, Table 4.3). However, the ^{1}MLCT bands of the analogous homodinuclear complexes of Os (**2** and **6**) are accompanied by the additional triplet-based ^{3}MLCT transitions within the range $13850 < \overline{\nu} < 16950$ cm^{-1} ($590 < \lambda < 720$ nm, Table 4.3). Heterodinuclear complexes **4** and **5** show both singlet- and triplet-based MLCT transitions (Table 4.3) with the ^{3}MLCT type due to the Os metal centre.

	Absorption peaks / cm^{-1} (nm)
1	23250, sh (430); 22222 (450)
2	22574, sh (443); 21375 (468, λ_{MAX}); 16937, b(590); 15378, sh (650)
3	23127, sh (432); 22160 (451, λ_{MAX})
4	22422, b (446, λ_{MAX}); 21231, b, sh (471); 17331, b (577); 14956, b, sh (668)
5	23567, sh (424); 21978 (455, λ_{MAX}); 20243, sh (494); 16313, b (613); 14298, b (700)
6	22260, b (449); 19960 (501, λ_{MAX}); 15385, b (650); 14045, sh (712)
7 [12d]	30303 (330, λ_{MAX}); 27174, sh (368); 22624, b (442); 20747, b (482)
8 [12e]	22123 (452)[a]
9 [12e]	25380 (394); 21786(459); 16666 (600); 15150 (660)
10 [12e]	25380 (393); 442, 21786 (460); 475; 16666 (600); 15150 (660)
11 [12e]	22123 (453); 17240 (580); 14925 (670)
12a [33b]	34965 (286); 22260 (448)
12b [33b]	34965 (289); 21231 (471); 15385 (650)
13a [34, 35]	40985 (244); 34845 (287); 22472 (445); 21231 (471)
13b [35]	19608 (510); 16129 (620)
14 [36]	40000 (250); 34965 (286); 22222 (450)

Table 4.3: *Spectral data for complexes **1** – **6** in acetonitrile; b: broad, sh: shoulder. Spectral data of the binuclear analogues **7** - **14** are included for comparison. a: only λ_{max}.The values in parentheses represent the wavelengths of the absorption peaks. Error = ±1 nm.*

The ^{3}MLCT bands are observed in the spectra of complexes containing osmium due to the stronger interaction of the electron spin with its orbital motion through spin orbit coupling (the greater the positive charge in a nucleus, the faster the electrons will orbit; therefore the interaction between electric currents and magnetic field will be stronger).[25] In ruthenium complexes these processes are classified as *spin - forbidden* and are not observed. When metal centred oxidation of binuclear species **1-6** is carried out significant changes to their electronic absorption spectra are seen with new bands within the range $7590 < \bar{\nu} < 17700$ cm^{-1} ($560 < \lambda < 1350$ nm) and the accompanying

decrease of the main MLCT absorption bands (**Error! Reference source not found.** to Figure 4.20).

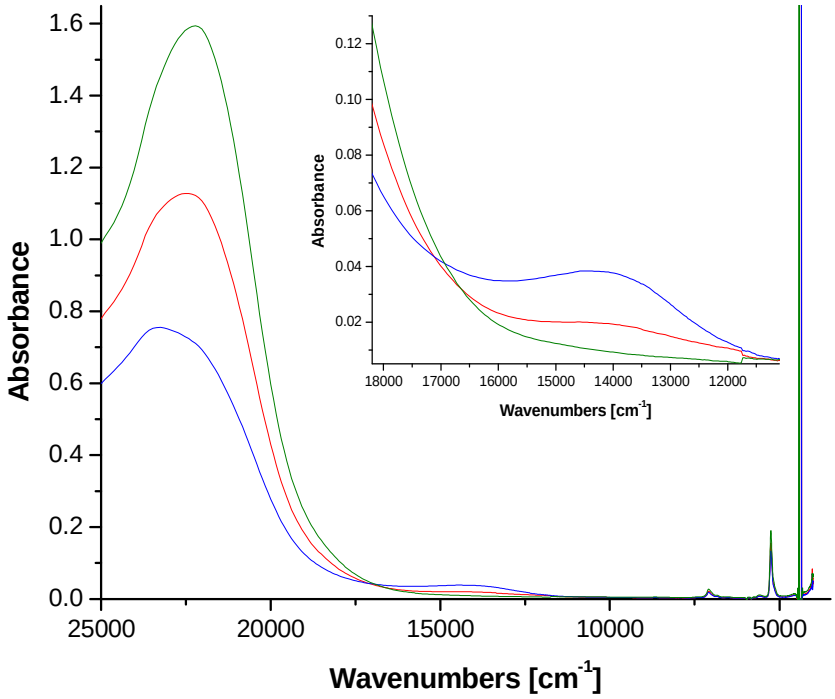

Figure 4.15: *Spectral variations of $[(bipy)_2Ru(qpy)Ru(bipy)_2]^{4+}$ (**1**) upon controlled electrochemical oxidation of Ru centres; 0.1 M $TBAPF_6$ in acetonitrile. (green) E = +0.30 V vs. SCE; (red) E = +1.33 V vs. SCE $[Ru^{III}Ru^{II}]$; (blue) E = +1.50 V vs. SCE $[Ru^{III}Ru^{III}]$. Inset: focusing on the region of 18200 – 11100 cm^{-1}.*

Spectroelectrochemical analysis of $[Ru(bpy)_2(qpy)Ru(bpy)_2]^{4+}$ (**1**) reveals that the region of most interest is the UV/Vis region where the ^{1}MLCT transitions of this complex absorb around 22200 cm^{-1} (450 nm), Figure 4.15. Since both metal centres in the complex are coordinated to strong π-acceptor ligands, the observed ligand to metal charge transfer (LMCT) bands are high in energy as a result of poor electron density on the bipyridyl rings. Such LMCT bands are observed at shorter wavelengths in the spectrum generally in the region of 25000-10000 nm.[49] The first of these occur at high energies, centred upon 23250 cm^{-1} (430 nm), and are not observed until the complex is fully oxidised as they are somewhat masked by the ^{1}MLCT absorption bands in the mixed valence and fully reduced states. The second set of LMCT transitions exhibit an

absorption band found in the region of 16600-12500 cm^{-1}. This is a very broad band of low intensity – characteristic of bipyridyl LMCT absorptions, Figure 4.15.

The symmetry across the bis-bipyridyl bridge in complex **1** leads to the simultaneous oxidation of the metal centres, $E_{1/2}$ = +1.34 V. The ^{1}MLCT peak is not observed in the fully oxidised $Ru^{III}Ru^{III}$ state and upon reduction to the $Ru^{II}Ru^{II}$ state this band reappears in the spectrum demonstrating the reversibility of the system. The decrease when going from the reduced state to the mixed valence $Ru^{III}Ru^{II}$, and finally, oxidised state is linear. Likewise, for the case of the LMCT band (16600 > $\bar{\nu}$ > 12500 cm^{-1}) the increase when oxidising from the fully reduced state, through the mixed valence state and on to the fully oxidised state is relatively linear. There is a baseline shift in the spectrum which will alter the linearity of the rate of change of the MLCT and LMCT absorption bands. Through analysis of the entire spectrum, looking further into the Near-IR region, it is noted that no additional bands appear which may be assigned as IT bands. This result and the analysis of the comproportionation constant, leave little evidence of any interaction between the two ruthenium metal centres in the mixed valence state. If there was interaction an IT band would be expected to appear in the Near-IR region.

From 10000 cm^{-1} through to 4000 cm^{-1}, any increase or decrease in signal is due to a baseline shift. It is also observed that water is being absorbed by the system, shown by the bands at 7246, 5235 and 4525 cm^{-1} (1380, 1910 and 2210 nm respectively).

$[Os(bipy)_2(qpy)Os(bipy)_2]^{4+}$ (**2**), the osmium analogue of **1**, was fully oxidised by bulk electrolysis, with the voltage held at +1.20 V (*vs.* SCE) followed by partial reduction (voltage at +0.89 V) in order to investigate the spectral properties of the mixed valence state. Both ^{1}MLCT (21270 cm^{-1} (470 nm)) and ^{3}MLCT (19230 > $\bar{\nu}$ > 13330 cm^{-1}) absorption bands are observed for **2**, Figure 4.16, with the ^{3}MLCT arising due to the increased spin-orbit coupling effect of the heavier osmium atom.

Oxidation of the Os complex **2** leads to the decrease of the MLCT absorption bands (Figure 4.16) and the simultaneous appearance of low intensity bands in the region 4450 < $\bar{\nu}$ < 5700 cm^{-1}. These weakly absorbing, low energy LMCT signals are

characteristic of osmium complexes.[50] They are assigned as Os^{III} dπ – dπ transitions and occur as a result of the larger spin-orbit coupling that can be found in osmium complexes.[51] Following bulk oxidation of the complex the system was partially reduced to obtain the mixed valence $Os^{III}Os^{II}$ state ($E_{1/2\ ox}$ = +0.89 V).

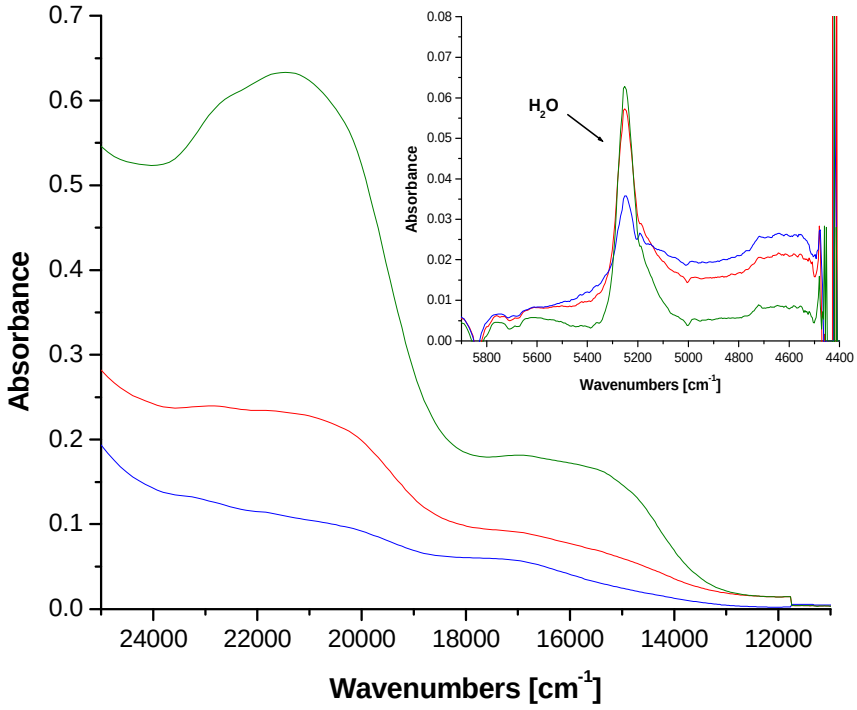

Figure 4.16: *Spectral variations of $[(bipy)_2Os(qpy)Os(bipy)_2]^{4+}$ (**2**) upon controlled electrochemical oxidation of Os centres; 0.1 M $TBAPF_6$ in acetonitrile. (green): E = +0.30 V vs. SCE; (red) E = +0.89 V vs. SCE [$Os^{III}Os^{II}$]; (blue) E = +1.20 V vs. SCE [$Os^{III}Os^{III}$]. Inset: focusing on the region of 5700 – 4400 cm^{-1}.*

The rate of change of absorbance from the fully oxidised to partially oxidised states is not a linear process. This absence of linearity as well as the lack of isospestic points may indicate possible electronic interaction between the metal centres in the mixed valence state. However, there are no intervalence bands observed which are required in order to conclusively state that an interaction occurs. The low energy LMCT bands observed in the mixed valence state also appear when the system is fully oxidised proving that they may not be assigned to intervalence bands as these types of interaction bands are not observed when complete oxidation is achieved. These results

show that any interaction between the metal centres is negligible and may be classed as a Type I interaction.

The spectroelectrochemistry of $[Ru(bipy)_2(qpy)Ru(bipy)_2]^{4+}$, **1**, and its osmium analogue (**2**) portrays no evidence of an electronic interaction between the metal centres in the mixed valence state. Varying the bridging ligand can strongly affect the electronic interaction between two metal centres in a dinuclear complex: the energies of the metal HOMO and LUMO levels can be adjusted as a consequence of changing the electronic properties of the bridging ligand. This was investigated with the introduction of a triazole moiety into the bridge in complex $[Ru(bipy)_2(pytr\text{-}bipy)Ru(bipy)_2]^{3+}$ (**3**). Triazoles exhibit strong σ-donor properties and give rise to a negative charge on the bridging ligand; the level of t_{2g} back bonding from the metal centre coordinated to the triazolato unit of the bridge is reduced leading to a less positive oxidation potential compared to complex **1**.

Upon oxidation of $[(bipy)_2Ru(pytr\text{-}bipy)Ru(bipy)_2]^{3+}$ (**3**) at +1.10 V *vs* SCE, the formation of a mixed valence species is recognisable through a decrease in the intensity of the ^{1}MLCT band (distinguishing between the ^{1}MLCT from the $[Ru(bipy)_2(pytr)]$ metal centre and the ^{1}MLCT from the $[Ru(bipy)_2(bipy)]$ metal centre), and with the appearance of a new band at around 11700 cm^{-1}, Figure 4.17. This is assigned as an LMCT absorbance band and not an IT band since it persists in the spectrum of the fully oxidised species also. This LMCT band is most likely due to the charge transfer from the pyridine-triazole moiety of the BL since the triazole ring possesses the stronger σ-donor properties with respect to pyridyl rings.[6a, 12e, 52]

The oxidation of the second metal centre at +1.40 V *vs* SCE brings about a further decrease in the ^{1}MLCT absorbance and an increase in intensity of the LMCT bands. Intervalence charge transfer bands are not observed in the spectrum of **3**, which indicates negligible communication between the metal centres in the mixed valence state despite the large value of K_c (1.8×10^6, Equation 4.11), confirming that separation is due to the asymmetry of the redox centres.[13] Therefore, $[Ru(bipy)_2(pytr)]^{2+}$ metal centre is oxidized first, with the $[Ru(bipy)_2(bipy)]^{2+}$ metal centre being oxidized thereafter (Figure 4.17).

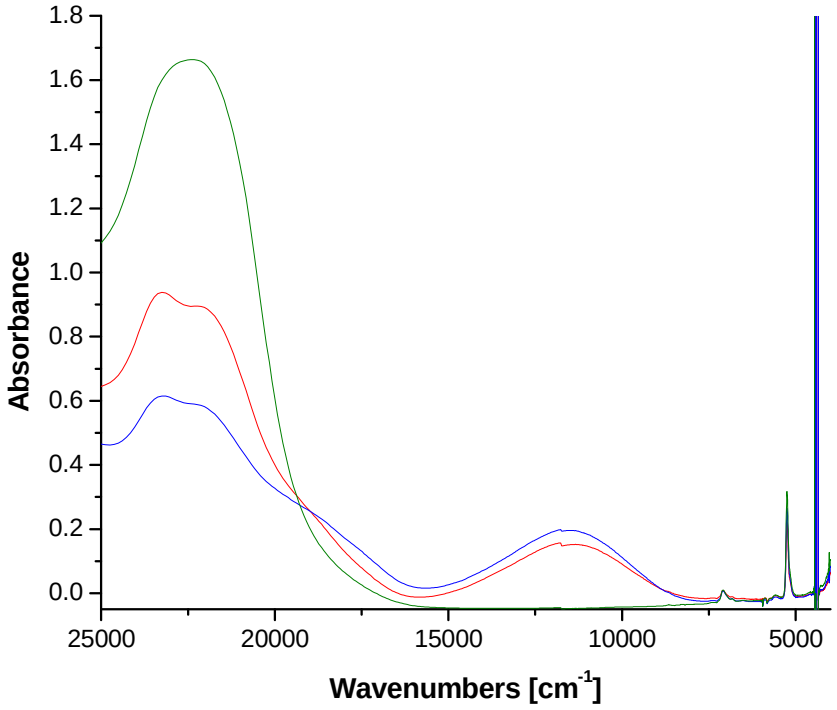

Figure 4.17: *Spectral variations of* $[(bipy)_2Ru(pytr\text{-}bipy)Ru(bipy)_2]^{3+}$ ***(3)*** *upon controlled electrochemical oxidation of Ru centres; 0.1 M* $TBAPF_6$ *in acetonitrile. (green): E = +0.30 V, vs. SCE; (red) E = +1.10 V vs. SCE* $[Ru^{III}Ru^{II}]$*; (blue) E = +1.40 V vs. SCE* $[Ru^{III}Ru^{III}]$*.*

The effect of the nature of the metal centre on the intramolecular interaction across the bridging ligand is investigated in the spectroelectrochemistry of heterodinuclear complexes **4** and **5**. The cyclic voltammetry of $[Ru(bipy)_2(pytr\text{-}bipy)Os(bipy)_2]^{3+}$ (**4**) shows two metal centred anodic processes occurring at potentials quite close to one another ($E_{1/2\ ox}$ = +0.86 and +0.97 V). Based on electrochemical analysis alone, it is not safe to assume that the osmium metal centre will be oxidised before the ruthenium metal centre due to the fact that the osmium is coordinated to the bipyridyl moiety of the bridge with the ruthenium coordinated to the pyridine-triazole section. As triazoles display much stronger σ-donor properties than bipyridyl ligands, therefore lowering the oxidation potential of the metals bonded to them, it is not possible to assign the oxidation potential of each metal without the aid of spectroelectrochemical analysis.

Bulk electrolysis of **4**, at a potential of +0.95 V *vs* SCE, (i.e. half way between the oxidation potentials of the two metal centres) results in a decrease in the intensity of the ^{1}MLCT and ^{3}MLCT absorptions. These results indicate that the [Os(bipy)$_2$(bipy)] metal centre is oxidized first due to the disappearance of the ^{3}MLCT transition. Furthermore, LMCT absorption bands are observed centred at ca. 11800 cm^{-1}, Figure 4.18. By increasing the applied potential to +1.10 V the oxidation of the second metal centre results in a further decrease of the ^{1}MLCT absorption band. A substantial increase in the intensity of the LMCT band occurs also, which is consistent with the donation of electron density from the triazole on the bridge to the Ru^{III} to stabilise the metal centre following oxidation.

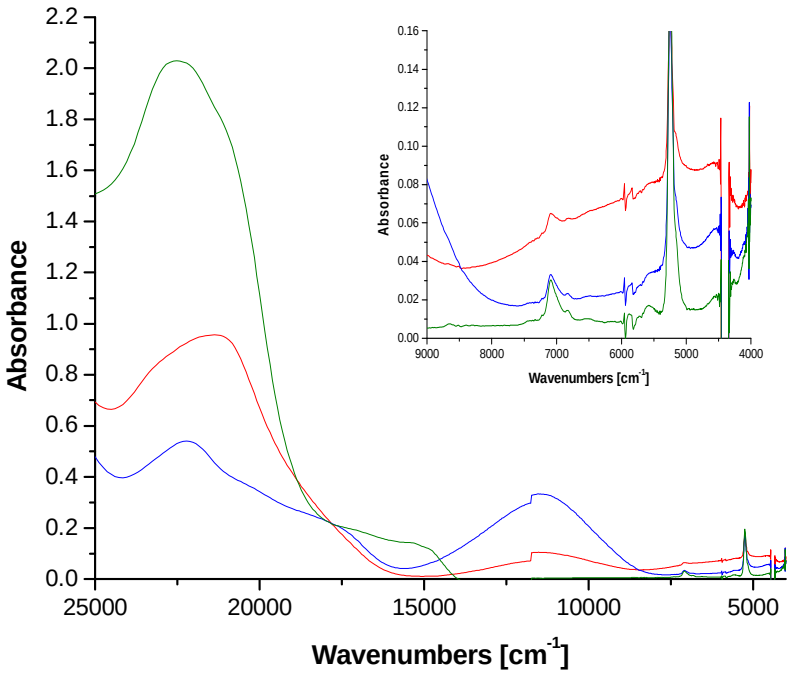

Figure 4.18: *Spectral variations of [(bipy)$_2$Ru(pytr-bipy)Os(bipy)$_2$]$^{3+}$ (**4**) upon controlled electrochemical oxidation of Os and Ru centres; 0.1 M TBAPF$_6$ in acetonitrile. (green): E = +0.30 V vs. SCE; (red) E = +0.95 V vs. SCE [Os^{III}-Ru^{II}]; (blue) E = +1.10 V vs. SCE [Os^{III}-Ru^{III}]. Inset: focusing on the region of 9000 – 4000 cm^{-1}.*

The mixed valence Ru^{II}Os^{III} absorbance spectrum of **4** reveals the formation of an IT band, Figure 4.18. This IT band is centred upon 5500 cm^{-1} and is a broad band of low intensity. This band is not observed in the fully oxidised Ru^{III}Os^{III} state leading to the

conclusion that it is in fact an IT band and not a low energy LMCT band. This coupled with the shape and height of the band would suggest that a Type II interaction is present between the metal centres in complex **4**.

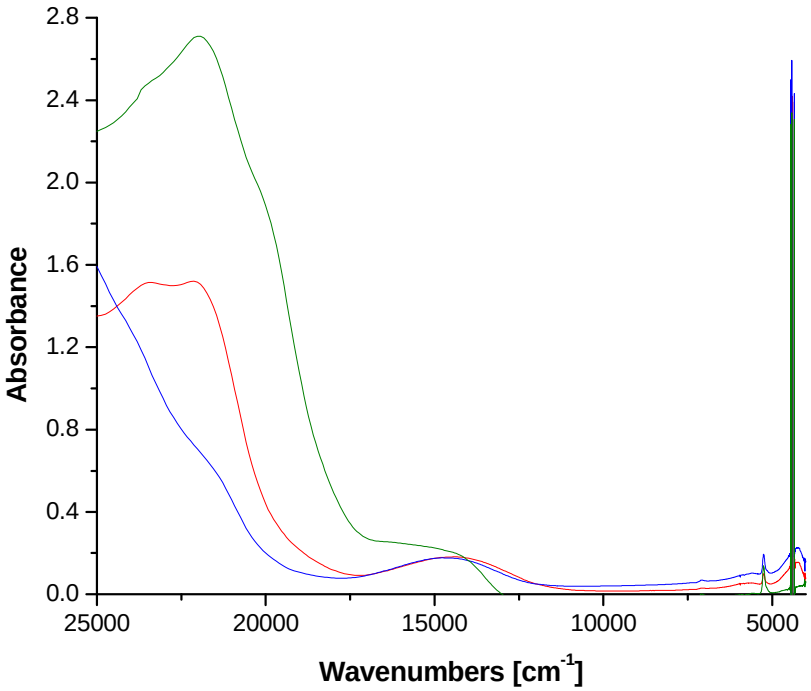

Figure 4.19: *Spectral variations of $[(bipy)_2Os(pytr\text{-}bipy)Ru(bipy)_2]^{3+}$ (**5**) upon controlled electrochemical oxidation of Os and Ru centres; 0.1 M $TBAPF_6$ in acetonitrile. (green) E = +0.30 V vs. SCE; (red) E = +0.90 V vs. SCE $[Os^{III}Ru^{II}]$; (blue) E = +1.50 V vs. SCE $[Os^{III}Ru^{III}]$.*

In contrast to **4** cyclic voltammetry of $[Os(bipy)_2(pytr\text{-}bipy)Ru(bipy)_2]^{3+}$ (**5**) reveals two well defined oxidations that exhibit a large peak – peak separation between them ($\Delta E_{1/2}$ = 750 mV). The higher energy of the 5d electrons in osmium metal complexes compared to ruthenium analogues results in a less positive oxidation potential of the former metal centres.[9] As a result of this, and the fact that the osmium metal centre in **5** is coordinated to a triazolato unit of the bridging ligand (a stronger σ-donor ligand than the bipyridyl ligand) it is assumed that the $[Os(bipy)_2(pytr)]$ metal centre is oxidized first, $E_{1/2\ ox}$ = +0.56 V, with the $[Ru(bipy)_2(bipy)]$ metal centre oxidised at a more positive potential, $E_{1/2\ ox}$ = +1.31 V.

The oxidation of **5** at +0.90 V *vs.* SCE results in the decrease in intensity of the ^{1}MLCT signal (Figure 4.19). It is also noted that the ^{3}MLCT band disappears and is replaced by an LMCT band centred at 14300 cm^{-1}. This confirms that the [Os(bipy)$_2$(pytr)] metal centre is oxidized first as expected from analysis of the electrochemical data (Figure 4.12, *vide supra*). The [Ru(bipy)$_2$(bipy)] metal centre is oxidised by bulk electrolysis (voltage at +1.50 V *vs.* SCE). This event is accompanied by a further decrease in the ^{1}MLCT bands (Figure 4.19). A second absorption band is observed in the mixed valence Os^{III}Ru^{II} state which appears in the low energy region of the spectrum at approximately 4300 cm^{-1}. This low energy broad LMCT band is characteristic for osmium (III) complexes. [53] This is observed in the fully oxidised Os^{III}Ru^{III} state thus indicating that it is an LMCT band and not an IT band. IT bands are not observed suggesting that interaction between the metal centres is negligible.

[Os(bipy)$_2$(pytr-pytr)Os(bipy)$_2$]$^{2+}$ (**6**) exhibits two sets of MLCT bands in the UV-vis-NIR spectrum (Figure 4.20). The ^{1}MLCT bands are centred at 20000 cm^{-1} (500 nm) while the ^{3}MLCT bands are centred at lower energies, i.e. 14900 cm^{-1} (670 nm). The half-wave potential of the first osmium metal centre is +0.47 V and +0.56 V *vs.* SCE for the second centre (Figure 4.14, *vide supra*). When the system is fully oxidised at +0.75 V *vs.* SCE the intensities of both ^{1}MLCT and ^{3}MLCT bands are reduced. An absorption band is observed at 13700 cm^{-1} (730 nm), that may be assigned to a bipyridyl-based LMCT transition as these π-acceptor ligands usually give rise to broad high energy bands.[49] The exact potential of the mixed valence state, half way between the oxidation potentials of the two metal centres, is not entirely clear from the cyclic voltammogram. A voltage of +0.51 V was selected as the point at which interaction, if any, would occur between the metal centres in the mixed valence state. The rate of change of the ^{1}MLCT band from the fully reduced species to the fully oxidised species is linear. The ^{3}MLCT also decreases linearly, however the ^{3}MLCT becomes masked by the LMCT when the system is fully oxidised which obscures the rate of change in the ^{3}MLCT peak. The fact that the LMCT band does not increase at the same rate as the MLCT bands decrease suggests that there may be an interaction between the two metal centres in the Os^{III}Os^{II} mixed valence state. At +0.51 V *vs* SCE when the system is partially oxidised LMCT absorption bands appear in the region of 12500 < $\bar{\nu}$ < 16600 cm^{-1}, Figure 4.20. Also, a very broad low intensity peak is observed in the

region of 4700 < $\bar{\nu}$ < 11100 cm^{-1} for the mixed valence state of **6**. This absorption is not observed for the fully oxidised form, indicating that these features are IT in nature.

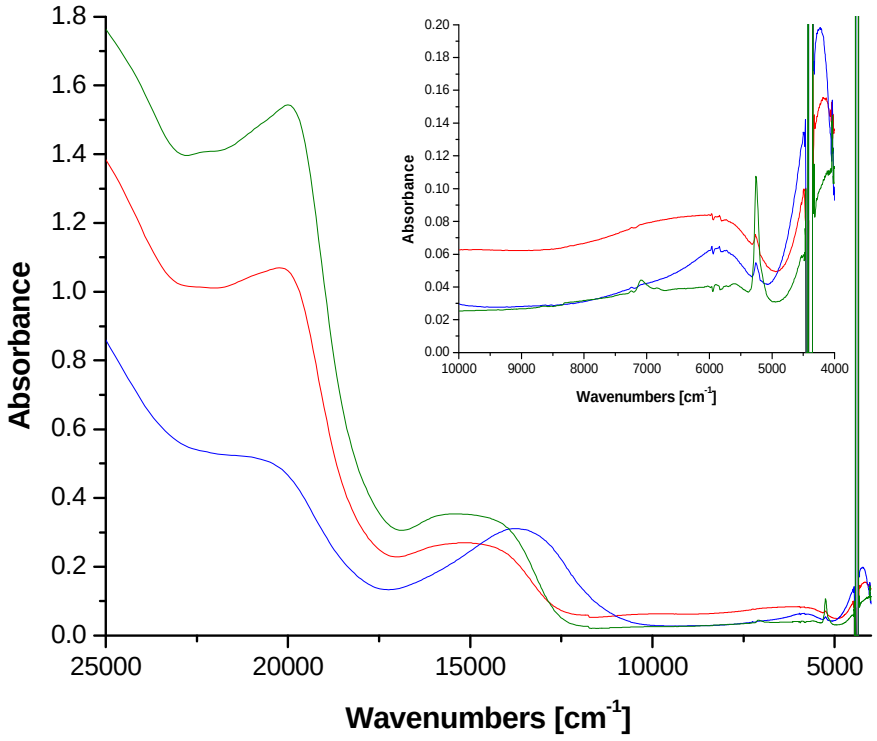

Figure 4.20: *Spectral variations of $[(bipy)_2Os(bpbt)Os(bipy)_2]^{2+}$ (**6**) upon controlled electrochemical oxidation of Os centres; 0.1 M $TBAPF_6$ in acetonitrile. (green) E = +0.30 V vs. SCE; (red) E = +0.51 V vs. SCE $[Os^{III}Os^{II}]$; (blue) E = +0.75 V vs. SCE $[Os^{III}Os^{III}]$. Inset: focusing on the region of 10000 – 4000 cm^{-1}.*

In the region of 5000 < $\bar{\nu}$ < 6900 cm^{-1} a new band is observed for the $Os^{(III)}Os^{(III)}$ state of complex **6** and it is assigned to an LMCT transition since it is no longer observed when the system is brought back to the fully reduced state $Os^{(II)}Os^{(II)}$. The mixed valence state shows a band of different shape and greater intensity in the same region as this LMCT band. The increase in intensity again suggests that there is an IT band in this region that may be masking the LMCT band that would be of weaker intensity in the mixed valence state. Analysis of the low energy region 4000 < $\bar{\nu}$ < 5000 cm^{-1} shows additional LMCT bands. The spectra for both states $Os^{III}Os^{II}$ and $Os^{III}Os^{III}$ of

complex **6** exhibit these LMCT peaks, being stronger for fully oxidised species. This indicates that these particular bands are LMCT and not IT bands in origin.

Overall, it is apparent that there is an interaction between the two metal centres of **6** in the mixed valence state. This is supported by the lack of isospestic points in the spectra. This interaction is small as indicated by the low intensity and broadness of the putative IT band.[54] The low intensity of the proposed IT band renders the evaluation of the various interaction parameters difficult (*vide infra*).[13, 17, 18, 19, 20a, 54]

4.2.4 Interaction Parameters in Mixed Valence States

The calculation of the equilibrium constant K_c through Equation 4.11 for the comproportionation reaction of Equation 4.8 allows for an evaluation of how displaced the reaction is towards the formation of a mixed valence product starting from a complex with fully oxidised metal centres and a complex with metal centres at their lower oxidation state.[47] This calculation relies on purely thermodynamic considerations since only the difference in oxidation potentials for the two metal centres (ΔE) of the binuclear complex is included in the formula (Equation 4.11).[13, 47] Consequently, K_c values cannot be indicative of the effective delocalisation of charge between the metal centres in the mixed valence compound.[13]

The four primary classifications for the electronic character of mixed valence dinuclear complexes are (i) type I (non-interacting), (ii) type II (weakly interacting), (iii) type II/III (solvent dependent interaction) and (iv) type III (strong interaction).[20] Depending on the extent of interaction between the metal centres in the mixed valence state, the delocalisation across both metal centres (α^2) and the electronic coupling H_{ab} between the metal centres will vary. Since large values for ΔE do not necessarily imply strong internuclear interaction, *i.e.* a large value for α^2 or H_{ab}, the analysis of spectroelectrochemical data is critical in the evaluation of the extent of interaction between metal centres when the mixed valence species display absorption bands deemed to originate from an IT process (optical electron transfer).

In the present series of binuclear complexes **1**-**6** IT related bands are unambiguously identifiable in the cases of $[(bipy)_2Ru(pytr\text{-}bipy)Os(bipy)_2]^{3+}$ (**4**), and

$[(bipy)_2Os(bpbt)Os(bipy)_2]^{2+}$ (**6**) (*vide supra*) and for the complex $[(bipy)_2Ru(bpbt)Ru(bipy)_2]^{2+}$ (**7**) [12d]. The calculation of the interaction parameters α^2 (Equation 4.5), H_{ab} (Equation 4.6) and $\Delta\nu_{1/2calc}$ (Equation 4.7) representing the delocalisation parameter, the coupling constant and the calculated peak width at half height for the IT band, respectively,[13, 17-20] is feasible only for the heteronuclear complex **4**, since the IT band observed in the spectrum of **6** has a broad low intensity character and lies in the same region as the low energy LMCT bands (*vide supra*) precluding accurate evaluation of the peak width and intensity.

	E_{op} / cm^{-1}	$\Delta\nu_{1/2exp}$ / cm^{-1}	ε_{max} / M^{-1}cm^{-1}	$\Delta\nu_{1/2calc}$ / cm^{-1}	α^2 (± 0.002 x 10^{-3})
4	5128	4636	633	3405	2.7*10^{-3}
7 [12d]	5490	4690	1820	3060	7.0*10^{-3}
8 [12e]	5556	3300	2400	3341	16.0*10^{-3}
9 [12e]	7143	3800	1200	3650	7.0*10^{-3}
10 [12e]	8333	4500	460	4170	2.7*10^{-3}
11 [12e]	8772	4300	1140	3700	6.1*10^{-3}

Table 4.4: *Interaction parameters α^2 (Equation 4.5), $\Delta\nu_{1/2calc}$ (Equation 4.7) and $\Delta\nu_{1/2exp.}$ between metal centres for complex **4** (this work), and complexes **7-11** (taken from literature). Values of ε_{max} and λ_{max} of E_{op} are also reported for the characterization of the IT transition in these binuclear complexes.*

From the spectral data $\Delta\nu_{1/2calc}$ = 3405 cm^{-1}, α^2 = 2.7*10^{-3} and H_{ab} = 267 cm^{-1} for $[(bipy)_2Ru(pytr\text{-}bipy)Os(bipy)_2]^{3+}$ (**4**) and ε_{MAX} = 633 M^{-1} cm^{-1}, $\Delta\nu_{1/2}$ = 4636 cm^{-1}, E_{opt} = 5128 cm^{-1}, ΔE = 887 cm^{-1} are obtained assuming 9.5 Å [12d] as a value of electron transfer distance, Table 4.4. Since the calculation of α^2 incorporates the geometrical metal-to-metal distance and does not take into account the reduction in electron transfer distance due to strong mixing between metal orbitals and BL-based orbitals (*vide supra)* the resulting values represent the lower limit only of the actual value for the coupling constant.[54]

The difference between $\Delta\nu_{1/2calc}$ and $\Delta\nu_{1/2}$ classifies the type of interaction between metal centres. Where $\Delta\nu_{1/2calc}$ and $\Delta\nu_{1/2}$ correlate then the system is best described as Type II (valence localized) mixed valence compound according to Robin and Day classification.[19] If the experimental IT band is narrower than that predicted by Equation 4.7 then the complex is defined as a Type III valence delocalized system. In case of complex **4** the $\Delta\nu_{1/2}$ value determined by direct measurement of the IT band is larger than the theoretical value (Equation 4.7) indicating that the system is best described as Type II (valence localized).[13, 19] From Table 4.4 it is clear that the interaction in terms of delocalisation in **4** is close to complexes such as **9** in which the metals are separated by an electron rich triazolato ligand.

Complexes **3**-**5** all contain the same BL (pytr-bipy) with the metal centres varying (i.e. ruthenium *vs.* osmium). The variation of the redox properties of **3**, **5** and **4** are in the first instance due to the difference in the redox potentials of the ruthenium and the corresponding osmium units, and, secondly, the difference in the coordination properties of the pyridine-triazolato and bipyridyl components of the ditopic bridging ligand. The metal centre coordinated to the pyridine-triazole moiety of the bridge in **3** and **5** is oxidised first, whereas in complex **4** it is the metal centre coordinated to the bipyridine moiety which is first oxidised. In fact, an IT band, which indicates significant internuclear interaction, is only observed in the spectrum of **4**, and not for the other two pytr-bipy bridged complexes **3** and **5**. This is counter intuitive considering that for symmetric dinuclear compounds an increase in the separation between the first and second oxidation potential (ΔE) typically indicates increased interaction strength (where the separation is not due to electrostatic interactions or asymmetry). The internuclear separation between the metal centres precludes either electrostatic interaction or direct metal orbital overlap between the osmium(III) and ruthenium(II) metal centres. Based on this, and the observation that internuclear interaction only occurs when it is the metal centre bound to the bipyridine moiety of the bridge that undergoes the first oxidation, the interaction strength manifested in the IT absorption band can be ascribed to HOMO mediated superexchange interaction between the metal centres; the dominant interaction is that of a $d\pi(M^{III})$- π(L) mixing with π -orbital from bipyridyl moiety, and the through BL-HOMO hole transfer mechanism is assumed.[13]

By comparison of the reduction potentials of **4** with those of **1** and **2** (Table 4.1), it can be seen that the π* (LUMO) of BL in **4** is higher in energy than that of both **1** and **2**. This additional consideration leads to the conclusion that the mechanism of intermetallic interaction in **4** is preferably through a BL-HOMO mediated and not a BL-LUMO mediated superexchange process.

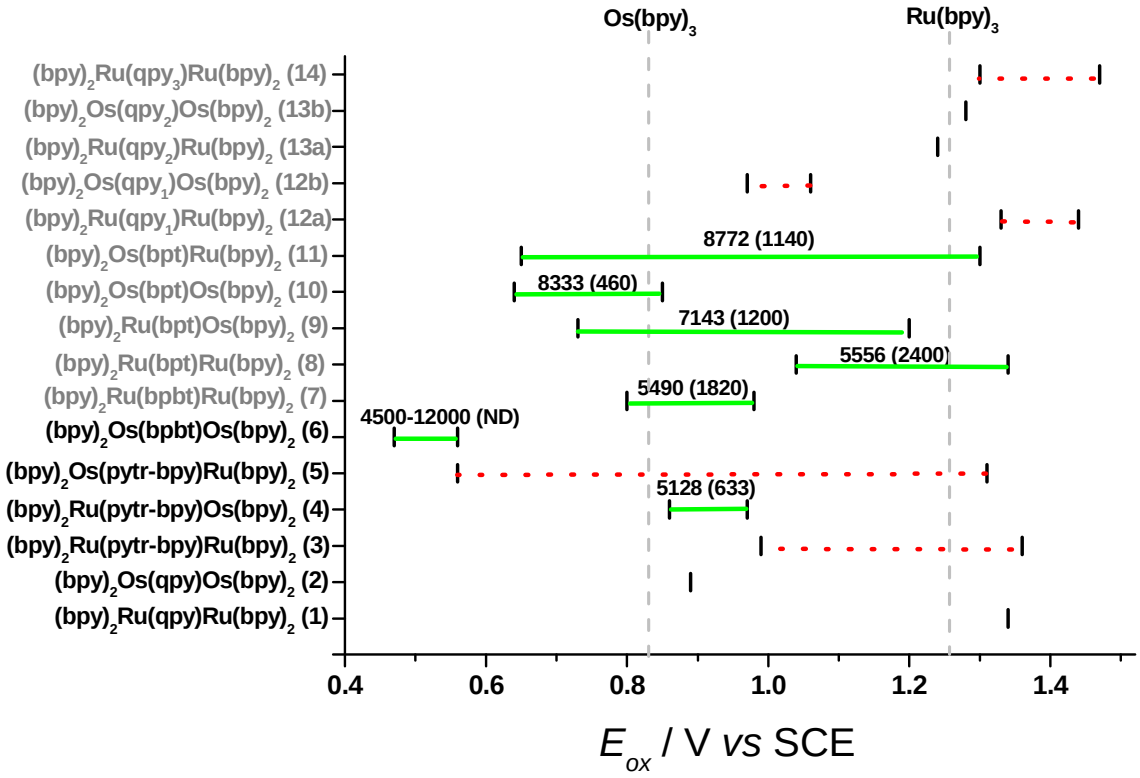

Figure 4.21: *Oxidation potentials for metal complexes **1-14**. Continuous/dotted lines indicate occurrence/lack of IT interaction between metal centres of the corresponding complex indicated on Y-axis. The values above the lines indicate the energy E_{op} (in cm^{-1}) of the IT absorption peak and in parentheses the molar absorptivity ε_{max} (in M^{-1} cm^{-1}) in correspondence of the IT peak. Oxidation potentials of $[Ru(bipy)_3]^{2+}$ and $[Os(bipy)_3]^{2+}$ are reported for reference.*

An important result emerging from the data reported in Figure 4.21 is the observation of IT transition only in case of $[(bipy)_2Ru(pytr\text{-}bipy)Os(bipy)_2]^{3+}$ (**4**) within the series of binuclear complexes **3-5** bridged by the same pytr-bipy ligand (Figure 4.7). The high specificity of the IT effect in one complex only within the series prompted the analysis of the mechanism of IT process in terms of the positions of frontier levels of

the metal centres and the ligands involved (Figure 4.22). The increased interaction observed for **4** compared with **3** and **5** can be rationalised by considering the nature of the optical electron transfer in terms of the energy of the "donor" and "acceptor" metal centres. For **4**, the optical transition, $Os^{III}Ru^{II} \rightarrow Os^{II}Ru^{III}$ involves a conversion to a state, which is relatively close in energy to the ground state compared with the corresponding transition for complex **3** and **5** (Figure 4.22). Furthermore, if an electron hopping model is considered then in the case of complexes **3** and **5** the optical transfer of an electron formally results in an increase in the energy difference of the HOMO orbitals of the bridging ligand (bpy- and pytr-) in the optically excited state whilst in the case of **4** these states move closer together in energy.

Homodinuclear complex **3** is characterized by having the first oxidation occurring at the ruthenium centre that coordinates the N atom of the triazole ring, Figure 4.11. In the mixed valence state of **3** it is expected that a partial negative charge is transferred from the pytr unit of the bridging ligand to the oxidised Ru centre as witnessed by the occurrence of the LMCT transition at 12000 cm-1, Figure 4.17. Such a transfer should lead to a lowering of the frontier levels of the pytr unit that then acquires a partial positive charge. It is supposed that the lowering of the HOMO level of pytr with a partial positive charge $\delta+$ is not sufficient to warrant a passage of electronic charge from the HOMO of the adjacent bipy unit.

Another possible reason for the missing charge transfer could be the scarce overlap between the orbitals of the different units constituting the bridging ligand (geometrical factor), but there is no apparent reason why such a geometrical effect would not be critical in case of complex **4**. Moreover, the occurrence of the MLCT transition between Ru(II) and the LUMO level of the bipy in the bridging ligand at 23000 cm-1 (Figure 4.17) is not followed by the energetically favourable transfer of charge between the LUMO level of the bipy and the LUMO level of the stabilized pytr with the $\delta+$ charge. This implies that possible IT in this type of complexes would occur only via a HOMO-mediated superexchange.

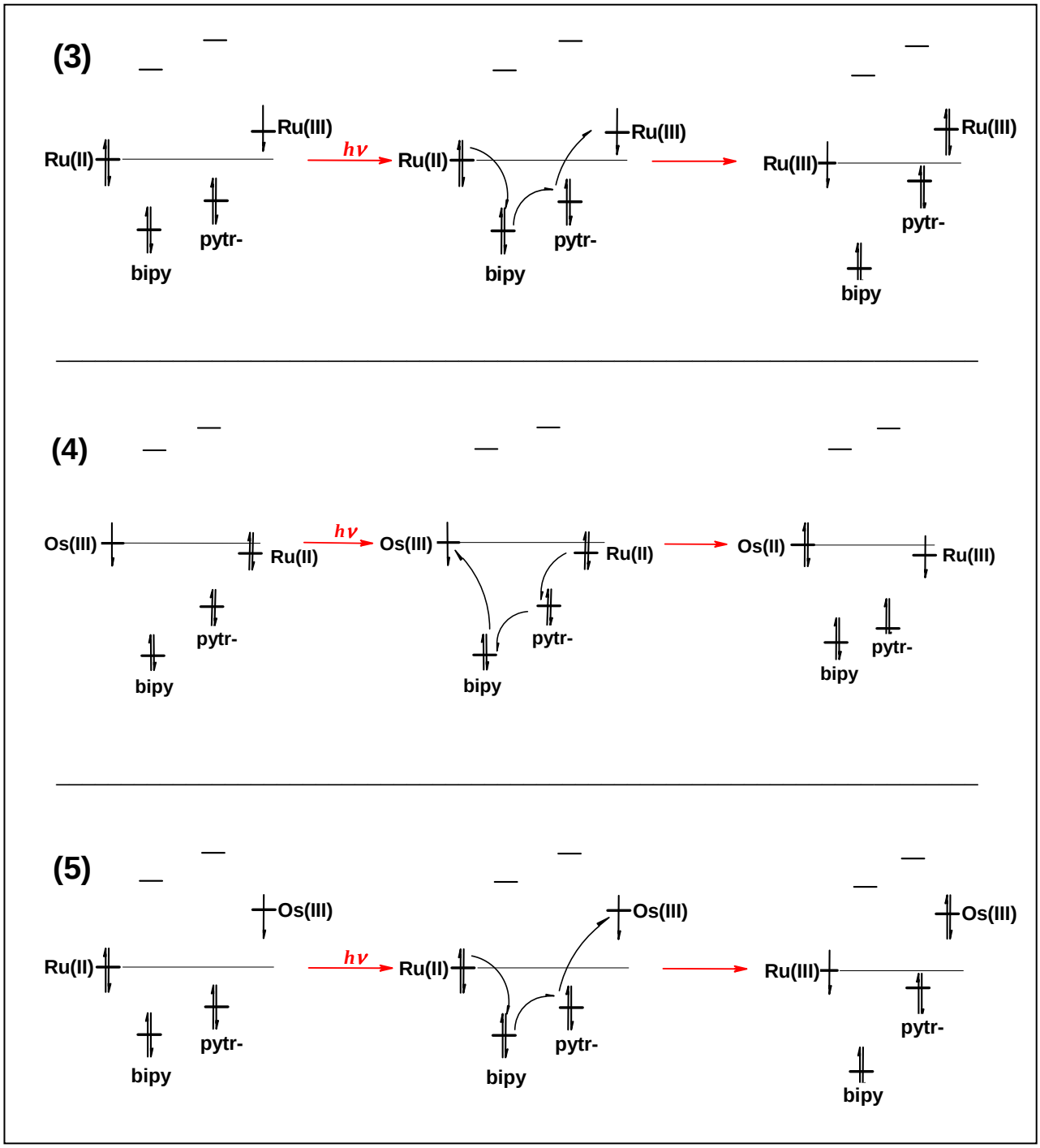

Figure 4.22: *Proposed mechanisms for the HOMO mediated superexchange in complexes **3** – **5** in the mixed valence states. The levels of the metal and ligand orbitals are relative energies only.*

Analogous considerations hold for the analysis of the impeded IT process in complex **5** where the Os centre is oxidized first. Neither charge transfers from bipy-HOMO to stabilized pytr δ+ HOMO and from bipy-LUMO to stabilized pytr δ+ LUMO take place after the MLCT transition between Ru(II) and the bipy unit of the bridging

ligand at 23000 cm^{-1}, and the LMCT transitions between the pytr unit of the bridging ligand and Os(III) at 14300 and 4300 cm^{-1}.

For the heterodinuclear complex **4**, intervalence bands are observed because, in contrast to **3** and **5**, the transfer of charge between the pytr- and bipy- units of the bridging ligand is energetically favourable via a HOMO mediated superexchange, Figure 4.22. In fact, the stabilization of the bipy orbitals following the LMCT between bipy unit and Os(III) at 13000 cm^{-1} is critical for the occurrence of the successive transfer of charge between the HOMO of the pytr unit and the stabilized HOMO (or SOMO) level of the partially positive δ+ bipy. As a rule it can be here established that IT will take place in those binuclear complexes in which the first oxidized metal centre is the one that coordinates the weaker electron donor N of the bridging ligand, usually the N atom of a bipy unit in polypyridyl systems.

Complexes **6** and **7** [12d] are bridged by the same bis-(pyridyl-triazolato) ligand but differ in the metal centres (*i.e.* osmium *vs.* ruthenium). The magnitude of ΔE for **6** is less and the intensity and energy of the IT band of the mixed valence state indicate that both the delocalisation (α^2) and interaction parameters H_{ab} possess lower values and hence the internuclear communication can be considered to be weaker. Previously, the interaction mechanism in the mixed valence state for complex **7** was assigned as being *via* HOMO mediated superexchange by the electron rich triazolato ligands. Hence the less positive oxidation potentials of the metal centres of **6** compared with **7** imply that mixing with the HOMO orbitals of the bridging ligand will be reduced: the greater distance from the dπ orbitals to the nucleus of the metal allows for less rigid movement of the 5d electrons and hence less mixing of the $d\pi(M^{III})$- π(BL) orbitals. This would explain the decreased interaction strength in **6**.

Figure 4.21 summarizes the spectroelectrochemical properties of complexes **1-14**. The first observation concerns the correlation between IT energies and relative position of the coordination sites of the interacting metals in the bridging ligand: the highest E_{op} of IT transitions are found for those complexes in which both metal centres coordinate N atoms from the same ring like the bpt bridged complexes **8-11** with E_{op} > 5500 cm^{-1}. The complexes in which the metal centres coordinate to sites belonging to adjacent

rings of the bridging ligand generally present lower values for E_{op} (< 5500 cm^{-1}), as verified with the bpbt bridged complexes **4** and **6**. This implies that the larger the distance between metal centres the greater the barrier for transfer of electron charge from one metal centre to another. Such a correlation is indicative of an electrostatic contribution, i.e. a through-space effect, controlling the energy of IT transition.

Another correlation for the complexes containing a triazole ring in the bridging ligand (complexes **4-11**), involves the intensity of the IT absorption, quantifiable with the ε_{max} parameter, and the nature of the metal centre that coordinates the N1 atom of the triazole in the bridging ligand. It is generally found that the higher values of ε_{max} for the IT transition are associated with those complexes having Ru (the more electronegative atom with respect to Os) coordinating the N1 atom of the triazole ring, i.e. the stronger σ-donor among the N atoms of the ring (complexes **7-9**). Such a correlation holds whether the triazole ring is shared (compounds **8-11**) or not (compounds **4-6**) by the two interacting metal centres. Another related observation is the direct proportionality between the value of the first potential of oxidation of dinuclear complexes displaying IT transition, and the intensity of this absorption through the evaluation of the ε_{max} value, i.e. the higher is $E_{1/2ox}$ the larger is ε_{max}. Since ruthenium oxidation occurs generally at higher potentials with respect to osmium, the dinuclear complexes with the more intense IT absorptions are expectedly those containing only ruthenium centres. Such a correlation is valid for complexes **7-9** in the order ε_{max} (**8**) > ε_{max} (**7**) > ε_{max} (**9**) being also $E_{1/2ox}$ (**8**) > $E_{1/2ox}$ (**7**) > $E_{1/2ox}$ (**9**), Figure 4.21. Within this series only complex **9** contains osmium when it coordinates the N4 of a triazole ring, i.e. a relatively poor electron donor atom of the triazole unit (Figure 4.7). We can conclude that if the first oxidized metal of a binuclear complex displaying IT absorption is ruthenium the IT absorption will be then characterized by a high intensity. Inversely, the weakest IT absorption bands appear when the osmium centre that coordinates the N1 of a triazole ring, i.e. the stronger electron donor atom of the ring, is first oxidized (complexes **6**, **10**, **11**, Figure 4.21).

4.3 Conclusions

The electrochemical properties of binuclear complexes **1** - **6** have been analysed and their spectroelectrochemical properties have been examined in the vis-NIR range. The oxidation potentials of the metal centres in quaterpyridyl bridged species **1** and **2** have a weak dependence on the type of quaterpyridyl isomer (compare complexes **12–14**), that bridges the two metal centres and oxidising the first metal centre shows no evidence of intermetallic communication in **1** and **2**. Within the group of pytr-bipy bridged complexes **3–5** only **4** exhibits spectroelectrochemical features in its mixed valence state, which could be assigned unambiguously to an IT transition. It is found that the overall change in energy involved in the IT transition (*i.e.* the difference in oxidation potentials of the metal centres), and the effect of the electron transfer on the relative energies of the HOMO orbitals associated with the binding units of the bridging ligand constitute the critical factors for the occurrence of IT; the structural factors that accompany such an electronic event within the studied series of complexes are the presence of osmium as metal centre, and the presence of at least one triazole moiety in the bridging ligand. In the sole case of **4** the ligand mediated electron transfer Ru(II)-[pytr-bipy]-Os(III) $\rightarrow$Ru(III)-[pytr-bipy]-Os(II) is possible because of the larger electron-withdrawing strength of the binding moiety (bipy) that is coordinated by the oxidised metal centre (Os). This implies a HOMO (of the bridging ligand) mediated superexchange mechanism where the energy differences between the HOMOs of the binding sites and the gap between these and the energy levels of the coordinating metals are the critical parameters.

Compound **6** displays an IT transition also, which occurs *via* a HOMO (of the bridging ligand) mediated superexchange mechanism. In the case of complexes **6** and **7** differing only in the nature of the metal centres, the weaker intermetallic interaction of osmium complex **6** in comparison to the analogous ruthenium complex **7** is due to the larger gap between the energy of the metal orbitals of Os with respect to Ru and the HOMO of the binding unit of the ligand. The delocalisation parameter, the coupling constant and the calculated peak width at half height could be evaluated only in the case of the heterodinuclear complex **4** since the IT band features of Os complex **6** were ill defined as a result of overlap with other types of electronic transitions in the same spectral region. Complex **4** can be considered of the Type II according to the

classification of Robin and Day, [19] i.e. a system that manifests properties originating from a relatively weak interaction between metallic centres as a result of a small perturbation of the isolated metal centres.

This series of homo- and heterodinuclear complexes exhibit electrochemical properties required for the development of molecular diodes in that they each have two stable redox centres that are electrochemically reversible and accessible at low potentials. In order to continue with the development of molecular diodes using these types of complexes a linker ligand is required so that they can be assembled to electrode(s). Following this, insertion into a nano-scale environment such as STM will allow for the measurement of the molecular conductivity and investigation of the interfacial electron transfer mechanisms.

4.4 Bibliography

1 (a) Lehn, J.M., *Agnew. Chem. Int. Ed.*, **1988**, *27*, 89. (b) Lehn, J.M., *Supramolecular Chemistry Concepts and Perspectives*, Wiley - VHC, Weinheim, Germany, **1995**.

2 Balzani, V., Credi, A., Venturi, M., *Molecular Devices and Machines - A Journey into the Nano World*, Wiley-VCH, Weinheim, Germany, **2003**.

3 (a) Balzani, V., Scandola, F., *Supramolecular Photochemistry*, Ellis Horwood, Chicester, UK, **1991**, (b) Balzani, V. Ed., *Supramolecular Photochemistry*, Reidel, Dordrecht, **1997**.

4 Balzani, V., Juris, A., Venturi, M., Campagna, S., Serroni, S., *Chem. Rev.*, **1996**, *96*, 759.

5 (a) Coe, B.J., Curati, N.R.M., *Comments Inorg. Chem.*, **2004**, *25*, 147, (b) Browne, W.R., O'Boyle, N.M., McGarvey, J.J., Vos, J.G., *Chem. Soc. Rev.*, **2005**, *34*, 641, (c) Balzani, V., Campagna, S., Denti, G., Juris, A., Serroni, S., Venturi, M., *Acc. Chem. Res.*, **1998**, *31*, 26, (d) Mirkin, C.A., Ratner, M.A., *Ann. Rev. Phys. Chem.*, **1992**, *43*, 719, (e) Todd, M.D., Mikkelsen, K.V., Hupp, J.T., Ratner, M.A., *New J. Chem.*, **1991**, *15*, 97, (f) Vos, J.G., Kelly, J.M., *Dalton Trans.*, **2006**, 4869.

6 (a) Juris, A., Balzani, V., Barigelletti, F., Campagna, S., Belser, P., Von Zelewsky, A., *Coord. Chem. Rev.*, **1988**, *84*, 85, (b) Kalyanasundaram, K., *Coord. Chem. Rev.*, **1982**, *46*, 159, (c) Demas, J.N., Taylor, D.G., *Inorg. Chem.*, **1979**, *18*, 3177, (d) Hager, G.D., Crosby, G.A., *J. Am. Chem. Soc.*, **1975**, *97*, 7031.

7 (a) Hissler, M., Harriman, A., Khatyr, A., Ziessel, R., *Chem.–Eur. J.*, **1999**, *5*, 3366, (b) Harriman, A., Romero, F.M., Ziessel, R., Benniston, A.C., *J. Phys. Chem. A*, **1999**, *103*, 5399, (c) Cleary, R.L., Byrom, K.J., Bardwell, D.A.,

Jeffery, J.C., Ward, M.D., Calogero, G., Armaroli, N., Flamigni, L., Barigelletti, F., *Inorg. Chem.*, **1997**, *36*, 2601, (d) Ruthkosky, M., Kelly, C.A., Castellano, F.N., Meyer, G.J., *Coord. Chem. Rev.*, **1998**, *171*, 309, (e) Tsushima, M., Ikeda, N., Yoshimura, A., Nozaki, K., Ohno, T., *Coord. Chem. Rev.*, **2000**, *208*, 299.

8 (a) Marcaccio, M., Paolucci, F., Paradisi, C., Roffia, S., Fontanesi, C., Yellowlees, L.J., Serroni, S., Campagna, S., Denti, G., Balzani, V., *J. Am. Chem. Soc.*, **1999**, *121*, 10081, (b) Stagni, S., Palazzi, A., Zacchini, S., Ballarin, B., Bruno, C., Marcaccio, M., Paolucci, F., Monari, M., Carano, M., Bard, A., *Inorg. Chem.*, **2006**, *45*, 695, (c) Marcaccio, M., Paolucci, F., Paradisi, C., Carano, M., Roffia, S., Fontanesi, C., Yellowlees, L.J., Serroni, S., Campagna, S., Balzani, V., *J. Electroanal. Chem.*, **2002**, *532*, 99, (d) Roffia, S., Casadei, R., Paolucci, F., Paradisi, C., Bignozzi, C.A., Scandola, F., *J. Electroanal. Chem.*, **1991**, *302*, 157.

9 Hage, R., *PhD. Thesis*, Leiden University, The Netherlands, **1991**.

10 Cotton, F.A., Wilkinson, G., Gaus, P.L., *Basic Inorganic Chemistry*, 3rd Ed., Wiley, New York, USA, **1995**.

11 (a) Gordon, K.C., Burrell, A.K., Simpson, T.J., Page, S.E., Kelso, G., Polson, M.I.J., Flood, A., *Eur. J. Inorg. Chem.*, **2002**, 554, (b) Demadis, K.D., Neyhart, G.A., Kober, E.M., Meyer, T.J., *J. Am. Chem. Soc.*, **1998**, *120*, 7121, (c) Haga, M., Matsumura-Inoue, T., Yamabe, S., *Inorg. Chem.*, **1987**, *26*, 4148, (d) D'Alessandro, D.M., Dinolfo, P.H., Davies, M.S., Hupp, J.T., Keene, F.R., *Inorg. Chem.*, **2006**, *45*, 3261.

12 (a) Hage, R., Dijkhuis, A.H.J., Haasnoot, J.G., Prins, R., Reedijk, J., Buchanan, B.E., Vos, J.G., *Inorg. Chem.*, **1988**, *27*, 2185, (b) Hage, R., Haasnoot, J.G., Reedijk, J., Wang, R., Vos, J.G., *Inorg. Chem.*, **1991**, *30*, 3263, (c) Hage, R., Lempers, H.E.B., Haasnoot, J.G., Reedijk, J., Weldon, F.M., Vos, J.G., *Inorg. Chem.*, **1997**, *36*, 3139, (d) Di Pietro, C., Serroni, S.,

Campagna, S., Gandolfi, M., Ballardini, R., Fanni, S., Browne, W.R., Vos, J.G., *Inorg. Chem.*, **2002**, *41*, 2871, (e) Hage, R., Haasnoot, J.G., Nieuwenhuis, H.A., Reedijk, J., De Ridder, D.J.A., Vos, J.G., *J. Am. Chem. Soc.*, **1990**, *112*, 9245, (f) Browne, W.R., O'Boyle, N.M., Henry, W., Guckian, A.L., Horn, S., Fett, T., O'Connor, C.M., Duati, M., De Cola, L., Coates, C.G., Ronayne, K.L., McGarvey, J.J., Vos, J.G., *J. Am. Chem. Soc.*, **2005**, *127*, 1229.

13 Browne, W.R., Hage, R., Vos, J.G., *Coord. Chem. Rev*. **2006**, *250*, 1653.

14 (a) Ward, M.D., Barigelletti, F., *Coord. Chem. Rev.*, **2001**, *216*, 127, (b) Beyeler, A., Belser, P., *Coord. Chem. Rev.*, **2002**, *230*, 29, (c) Richter, M.M., Brewer, K.J., *Inorg. Chem.*, **1993**, *32*, 2827, (d) Hughes, H.P., Vos, J.G., *Inorg. Chem.*, **1995**, *34*, 4001, (e) Schlicke, B., Belser, P., De Cola, L., Sabbioni, E., Balzani,V., *J. Am. Chem. Soc.*, **1999**, *121*, 4207, (f) Gholamkass, B., Nozaki, K., Ohno, T., *J. Phys. Chem. B*, **1997**, *101*, 9010, (g) Fellows, E.A., Keene, F.R., *J. Phys. Chem. B*, **2007**, *111*, 6667.

15 Richardson, D.E., Taube, H., *Coord. Chem. Rev.*, **1984**, *60*, 107.

16 De Cola, L., Belser, P., *Coord. Chem. Rev.*, **1998**, *177*, 301.

17 Creutz, C., *Progress of Inorganic Chemistry*, Ed. S. J. Lippard, Wiley, New York, USA, **1983**.

18 Creutz, C., Newton, M.D., Sutin, N.J., *J. Photochem. Photobiol. A*, **1994**, *82*, 47.

19 Robin, M.B., Day, P., *Adv. Inorg. Chem. Radiochem*, **1967**, *10*, 247.

20 (a) Hush, N.S., *Prog. Inorg. Chem.*, **1967**, *8*, 391, (b) Hush, N.S., *Electrochim. Acta*, **1968**, *13*, 1005.

21 (a) D'Alessandro, D.M., Keene, F.R., *Pure Appl. Chem.*, 2008, **80**, 1, (b) D'Alessandro, D.M., Keene, F.R., *Chem. Rev.*, **2006**, *106*, 2270, (c) Launay, J.P., *Chem. Soc. Rev.*, **2001**, *30*, 386.

22 Goldsby, K.A., Meyer, T.J., *Inorg. Chem.*, **1984**, *23*, 3002.

23 (a) D'Alessandro, D.M., Keene, F.R., *Chem. Soc. Rev.*, **2006**, *35*, 424, (b) Demadis, K.D., Neyhart, G.A., Kober, E.M., White, P.S., Meyer, T.J., *Inorg. Chem.*, **1999**, *38*, 5948.

24 Creutz, C., Taube, H., *J. Am. Chem. Soc.*, **1969**, *91*, 3988.

25 Browne, W.R., *Ph.D. Thesis*, Dublin City University, Ireland, **2002**.

26 (a) Bardwell, D., Jeffrey, J.C., Joulié, L., Ward, M.D., *Dalton Trans*., **1993**, 2255, (b) Ward, M.D., *Chem. Soc. Rev.*, **1995**, *24*, 121.

27 Van Diemen, J.H., Hage, R., Haasnoot, J.G., Lempers, H.E.B., Reedijk, J., Vos, J.G., De Cola, L., Barigelletti, F., Balzani, V., *Inorg. Chem.* **1992**, *31*, 3518.

28 (a) Barigelletti, F., De Cola, L., Balzani, V., Hage, R., Haasnoot, J.G., Reedijk, J., Vos, J.G., *Inorg. Chem.*, **1989**, *28*, 4344, (b) Barigelletti, F., De Cola, L., Balzani, V., Hage, R., Haasnoot, J.G., Reedijk, J., Vos, J.G., *Inorg. Chem.* **1991**, *30*, 641.

29 Browne, W.R., de Jong, J.J.D., Kuderac, T., Walko, M., Lucas, L.N., Uchida, K., van Esch, J.H., Feringa, B.L., *Chem. Eur. J.*, **2005**, *11*, 6414.

30 Cassidy, L., *Ph.D. Thesis*, Dublin City University, Ireland, **2008**.

31 Cassidy, L., Horne, S., Cleary, L., Halpin, Y., Browne, W.R., Vos, J.G., *Dalton Trans*., **2009**, 3923.

32 De Cola, L., Barigelletti, F., Balzani, V., Hage, R., Haasnoot, J.G., Reedijk, J., Vos, J.G., *Chem. Phys. Lett.*, **1991**, *178*, 491.

33 (a) Ward, M.D., *J. Chem. Soc. Dalton Trans.*, **1994**, 3095, (b) Balzani, V., Bardwell, D.A., Barigelletti, F., Cleary, R.L., Guardigli, M., Jeffery, J.C., Sovrani, T., Ward, M.D., *J. Chem. Soc. Dalton Trans.*, **1995**, 3601.

34 Downard, A.J., Honey, G.E., Phillips, L.F., Steel, P.J., *Inorg. Chem.*, **1991**, *30*, 2259.

35 Fang, Y.Q., Polson, M.I.J., Hanan, G.S., *Inorg. Chem.*, **2003**, *42*, 5.

36 Ward, M.D., *J. Chem. Soc. Dalton Trans.*, **1993**, 1321.

37 Baitalik, S., Dutta, B., Nag, K., *Polyhedron*, **2004**, *23*, 913.

38 Bardwell, D.A., Barigelletti, F., Cleary, R.L., Flamigni, L., Guardigli, M., Jeffery, J.C., Ward, M.D., *Inorg. Chem.*, **1995**, *34*, 2438.

39 Elliott, C.M., Hershenhart, E.J., *J. Am. Chem. Soc.*, **1982**, *104*, 7519.

40 (a) Saji, T., Aoyagui, S., *J. Electroanal. Chem.*, **1975**, *58*, 401, (b) Saji, T., Aoyagui, S., *J. Electroanal. Chem.*, **1975**, *60*, 1.

41 (a) Taube, H., *Pure Appl. Chem.*, **1979**, *51*, 901, (b) Kalyanasundaram, K., Nazeeruddin, M.K., *Chem. Phys. Lett.*, **1989**, *158*, 45, (c) Kalyanasundaram, K., Nazeeruddin, M.K., *Inorg. Chim. Acta*, **1990**, *171*, 213.

42 Hibbert, D.B., *Introduction to Electrochemistry*, Macmillan Press Ltd, London, UK, **1993**.

43 Sawyer, D.T., Sobkowiak, A., Roberts Jr., J. L., *Electrochemistry for Chemists*, 2nd Ed., John Wiley & Sons, USA, **1995**.

44 (a) Rillema, D.P., Mack, K.B., *Inorg. Chem.*, **1982**, *21*, 3849, (b) Cooper, J.B., MacQueen, D.B., Petersen, J.D., Wertz, D.W., *Inorg. Chem.*, **1990**, *29*, 3701.

45 (a) Browne, W.R., O'Connor, C.M., Hughes, H.P., Hage, R., Walter, O., Doering, M., Gallagher, J.F., Vos, J.G., *Dalton Trans,* **2002**, 4048, (b) Pappenfus, T.M., Mann, K.R., *Inorg. Chem.*, **2001**, *40*, 6301.

46 (a) Orellana, G., Quiroga, M.L., Braun, A.M., *Helv. Chim. Acta*, **1987**, *70*, 2073, (b) Hage, R., Haasnoot, J.G., Stufkens, D.J., Snoeck, T.L., Vos, J.G., Reedijk, J., *Inorg. Chem.*, **1989**, *28*, 1413.

47 Richardson, D.E., Taube, H., *Inorg. Chem.*, **1981**, *20*, 1278.

48 Juris, A., Campagna, S., Balzani, V., Gremaud, G., Von Zelewsky, A., *Inorg. Chem.*, **1988**, *27*, 3652.

49 Passaniti, P., Browne, W.R., Lynch, F.C., Hughes, D., Nieuwenhuyzen, M., James, P., Maestri, M., Vos, J.G., *J. Chem. Soc., Dalton Trans.*, **2002**, 1740.

50 Weldon, F., *Ph.D. Thesis*, Dublin City University, Ireland, **1998**.

51 Haga, M., Ali, M., Arakawa, R., *Angew. Chem. Int. Ed. Engl.*, **1996**, *35*, 76.

52 Duati, M., Tasca, S., Lynch, F.C., Bohlen, H., Vos, J.G., Stagni, S., Ward, M.D., *Inorg. Chem.*, **2003**, *42*, 8377.

53 Sauvage, J.P., Collin, J.P., Chambron, J.C., Guillerez, S., Coudret, C., Balzani, V., Barigelletti, F., De Cola, L., Flamigni, L., *Chem. Rev.*, **1994**, *94*, 993.

54 Demadis, K.D., Hartshorn, C.M., Meyer, T.J., *Chem. Rev.*, **2001**, *101*, 2655.